# Hammerhead-type FXR agonists induce an eRNA FincoR that ameliorates nonalcoholic steatohepatitis in mice

Jinjing Chen[a, #], Ruoyu Wang[b, #], Feng Xiong[b], Hao Sun[a], Byron Kemper[a], Wenbo Li[b,*] and Jongsook Kim Kemper[a,*]

[a]Department of Molecular and Integrative Physiology, University of Illinois at Urbana-Champaign, Urbana, IL, USA and [b]Department of Biochemistry and Molecular Biology, McGovern Medical School, University of Texas Health Science Center, Houston, TX, USA

Running Title: Role of an FXR-induced eRNA, FincoR, in NASH

[#]JC and RW contributed equally to this study.

Present Address: Jinjing Chen, Department of Pharmacology and Toxicology, University of Arizona, Tucson, AZ, USA

* To whom correspondence may be addressed:

* Wenbo Li, Department of Biochemistry and Molecular Biology, McGovern Medical School, University of Texas Health Science Center, Houston, TX, USA

Graduate School of Biomedical Sciences, University of Texas MD Anderson Cancer Center and UTHealth, Houston, TX, USA

Tel: 713-500-6103, e-mail: Wenbo.Li@uth.tmc.edu

* J. Kim Kemper, Department of Molecular and Integrative Physiology,

University of Illinois at Urbana-Champaign, Urbana, IL

Tel: 217-722-7961, e-mail: jongsook@illinois.edu

**Key words:** FXR, nuclear receptor, lncRNA, enhancer, enhancer RNA, tropifexor, hepatic inflammation, NASH, NAFLD, RNA-seq, Gro-seq

**Author Contributions:**

JC, RW, WL and JK designed research; JC, RW, FX, and HS performed experiments; RW and WL performed bioinformatic analyses; JC, RW, WL, and BK analyzed data; and JC, RW, BK, WL, and JK wrote the paper.

**Abstract**

The nuclear receptor, Farnesoid X Receptor (FXR/NR1H4), is increasingly recognized as a promising drug target for metabolic diseases, including nonalcoholic steatohepatitis (NASH). Protein coding genes regulated by FXR are well known, but whether FXR also acts through regulation of expression of long non-coding RNAs (lncRNAs), which vastly outnumber protein-coding genes, remains unknown. Utilizing RNA-seq and GRO-seq analyses in mouse liver, we found that FXR induces many RNA transcripts from chromatin regions bearing enhancer features. Among these we discovered a previously unannotated liver-enriched enhancer-derived lncRNA (eRNA), termed *FincoR*. We further show that *FincoR* is specifically induced by hammerhead-type FXR agonists, including GW4064 and tropifexor. CRISPR/Cas9-mediated liver-specific knockdown of *FincoR* in dietary NASH mice reduced the beneficial effects of tropifexor, an FXR agonist currently in clinical trials for NASH and primary biliary cholangitis (PBC), indicating that that amelioration of liver fibrosis and inflammation in NASH treatment by tropifexor is mediated in part by FincoR. Overall, our results indicate that pharmacological activation of FXR by hammerhead-type agonists induces a novel eRNA, *FincoR*, ameliorating NASH in mice. *FincoR* may represent a new drug target for combating metabolic disorders, including NASH.

68 **Introduction**

69 Nonalcoholic fatty liver disease (NAFLD) is the most common chronic liver disease and
70 a leading cause of liver transplants and liver-related death *(Friedman and Sanyal 2018)*.
71 NAFLD begins with simple steatosis but may further progress to a severe form, non-
72 alcoholic steatohepatitis (NASH), and later, fatal cirrhosis and liver cancer *(Friedman and*
73 *Sanyal, 2018)*. Despite its striking global increase and clinical importance, there is no
74 approved drug for NASH. The urgent need for development of therapeutic agents for
75 NASH has greatly increased research interest in the nuclear receptor, Farnesoid X
76 Receptor (FXR, NR1H4) *(Evans and Mangelsdorf, 2014)*.

77 FXR is activated by its physiological ligands, bile acids (BAs), and regulates
78 expression of genes involved in BA, lipid, and glucose metabolism and hepatic autophagy,
79 which maintains metabolite levels and metabolic homeostasis *(Lee et al., 2006; Calkin*
80 *and Tontonoz, 2012; Lee et al., 2014; Seok et al., 2014; Kliewer and Mangelsdorf, 2015)*.
81 Ligand-activated FXR also protects against hepatic inflammation and liver injury *(Wang*
82 *et al., 2008; Jung et al., 2020)*. The action of FXR, similar to other nuclear receptors, is
83 achieved primarily by binding to chromatin at specific gene loci to regulate the
84 transcription of target genes *(Lee et al., 2006; Thomas et al., 2010; Lee et al., 2012;*
85 *Calkin and Tontonoz, 2012)*. Consistent with its crucial physiological functions, FXR is
86 increasingly recognized as a promising drug target, particularly for liver diseases, such
87 as NASH and primary biliary cholangitis (PBC) *(Downes et al., 2003; Ali et al., 2015;*
88 *Abenavoli et al., 2018; Kremoser, 2021)*. For example, semi-synthetic or non-steroidal
89 synthetic agonists of FXR, including obeticholic acid (OCA) and hammerhead-type
90 agonists, such as tropifexor and cilofexor, are currently under clinical trials for NASH and

91 PBC patients *(Tully et al., 2017; Abenavoli et al., 2018; Kremoser, 2021; Sanyal et al.,*
92 *2023)*. However, how pharmacological activation of FXR mediates such beneficial
93 therapeutic effects is poorly understood.

94 Non-protein-coding RNAs (ncRNAs) are one of the fascinating discoveries of
95 modern biology *(Cech and Steitz, 2014)*. Indeed, only about 2% of the human genome
96 encodes proteins, while the vast majority are transcribed into ncRNAs *(The ENCODE*
97 *Project Consortium, 2012)*. Of these ncRNAs, long non-coding RNAs (lncRNAs) are a
98 group of transcripts longer than 200 nucleotides and play important roles in diverse
99 biological processes *(Lam et al., 2014; Li et al., 2016; Sartorelli and Lauberth, 2020;*
100 *Statello et al., 2021; Mattick et al., 2023)*. Many lncRNAs are produced from genomic
101 regions bearing epigenetic features of enhancers *(Hon et al., 2017; Mattick et al., 2023)*.
102 This is consistent with the idea that many transcriptional enhancers actively transcribe
103 noncoding RNAs that are referred to as eRNAs, some of which are functionally important
104 for enhancer functions *(Lai and Shiekhattar, 2014; Li et al., 2016)*. Due to the increasing
105 technical sensitivity of RNA detection, many enhancers have been found to produce
106 eRNAs (>85k in humans and >57k in mice) *(Hirabayashi et al., 2019)*. Many eRNAs have
107 not yet been annotated in current lncRNA databases, such as GENCODE. Exploring
108 eRNA landscapes and functions in diverse biology and disease states will facilitate our
109 understanding of both lncRNAs and enhancers *(Li et al., 2016; Mattick et al., 2023)*.
110 However, the landscape of eRNAs in mouse liver has been minimally explored *(Fang et*
111 *al., 2014)*, and has not been studied in response to specific nuclear receptor activation,
112 such as by FXR. Moreover, functional role of eRNAs in vivo in intact organisms is
113 understudied.

114 FXR was shown to regulate expression of small non-coding microRNA (miR)
115 genes, for example *miR-34a and miR-802 (Lee et al., 2010; Seok et al., 2021)*, but it has
116 not been reported whether FXR mediates its function through regulating lncRNAs, which
117 far outnumber miRs. Because FXR directly regulates expression of its target genes
118 *(Thomas et al., 2010; Lee et al., 2012)*, we examined if FXR regulates enhancer-derived
119 lncRNAs, and if such transcripts participate in its physiological or pharmacological
120 functions. By utilizing RNA-seq and GRO-seq analyses of mouse liver treated by FXR
121 ligands, we identified a series of FXR-regulated eRNAs, including many that were
122 previously unannotated. Among these, we focused on a highly induced and abundantly
123 expressed eRNA that we referred to as FXR-induced non-coding RNA (*FincoR*) for
124 functional studies. *FincoR* is highly enriched in mouse liver and is induced specifically by
125 hammerhead-type FXR agonists, including GW4064 and tropifexor. In vivo studies
126 utilizing CRISPR/Cas9-mediated liver-specific knockdown of *FincoR* in dietary NASH
127 mice indicated that *FincoR* is critically involved in mediating the beneficial
128 pharmacological effects of tropifexor in reducing liver fibrosis and inflammation.
129

130 **Results**

131 **Activation of FXR by GW4064 induces a novel eRNA, *FincoR*, in mouse liver**

132 To identify enhancer-derived lncRNAs (eRNAs) potentially regulated by FXR, we first
133 obtained a list of putative enhancers in mouse liver based on ENCODE H3K27ac ChIP-
134 Seq data (ENCFF001KMI, see **methods**). Then, we performed ribo-depleted total RNA-
135 seq in the livers from mice treated with a specific FXR agonist, GW4064, to identify
136 transcripts produced from these enhancer regions (see **Supplementary Table S1**). To

137 avoid confounding issues of RNA signals from genes, we specifically focused on
138 intergenic enhancer regions (+/- 3kb from H3K27ac peak center) that harbor discernible
139 RNA-Seq signals (RPKM > 1).

140 This genomic analysis resulted in identification of 190 high-confidence eRNAs in
141 mouse liver. Among these, 14 eRNAs were upregulated and 5 were downregulated by
142 GW4064 treatment (FDR < 0.05, Log2 FC > 1, **Figure 1A**) (see **Supplementary Table**
143 **S2**). FXR-regulated eRNAs were produced adjacent to many genes with important roles
144 in liver metabolism and disease, for example, *Hes1* (**Figure 1-Figure Supplement 1A,**
145 **B**). One of the most robustly induced eRNAs was *FXR-induced non-coding RNA*
146 (*FincoR)*, an unannotated novel transcript located on chromosome 19 (**Figure 1A, B, C**).
147 Reverse transcription qPCR (RT-qPCR) confirmed that treatment with GW4064
148 substantially induced expression of *FincoR,* more than 10-fold in mouse liver, which is
149 similar to induction of *Shp*, a well-known FXR target gene (**Figure 1D**) *(Goodwin et al.,*
150 *2000; Claudel et al., 2005; Evans and Mangelsdorf, 2014)*. Induction of *FincoR* by
151 GW4064 was transient, peaked within 1 h and then, declined gradually, similar pattern to
152 *Shp* (**Figure 1-Figure Supplement 1C**). Expression of genes adjacent to *FincoR*,
153 including *Gcnt1, Rfk, Pcsk5 and Prune2,* did not change after acute 1 h FXR activation
154 as shown by RNA-seq (**Figure 1C**), and confirmed for *Gcnt1* by time course qPCR
155 (**Figure 1-Figure Supplement 1C**).

156 We also found that the short GW4064 treatment resulted in 590 up-regulated
157 genes and 500 down-regulated genes (FDR < 0.05) (**Figure 1-Figure Supplement 2A**).
158 GO enrichment analysis of these differentially expressed genes (DEGs) revealed their
159 roles in the regulation of triglyceride, fatty acid, and cholesterol metabolism (**Figure 1-**

160 **Figure Supplement 2B**), which is consistent with known roles of FXR in these
161 physiological processes *(Claudel et al., 2005)*.
162
163 **Ligand-activated FXR directly activates transcription of eRNAs, including *FincoR.***
164 We sought to examine, 1) if these eRNAs were directly activated by FXR, and 2) if the
165 activation takes place transcriptionally using FXR liver-specific knockout (FXR-LKO) mice
166 that were treated with GW4064 to determine if FXR was required for induction of eRNAs
167 by GW4064. FXR-LKO mice were generated from FXR floxed mice (FXR-flox) **(Figure 2-**
168 **Figure Supplement 1A**) and transcription of eRNAs was detected by global run-on
169 sequencing (GRO-seq), a widely used method to detect nascent RNA transcription,
170 including eRNAs *(Lam et al., 2014; Li et al., 2016; Sartorelli and Lauberth, 2020)*. GRO-
171 seq showed that FXR-induced eRNAs were activated transcriptionally by GW4064 in
172 FXR-flox mice, but such induction was abolished in FXR-LKO mice (**Figure 2A**). In
173 particular, *FincoR* is robustly induced in the GRO-Seq analysis and its induction is
174 dependent on hepatic FXR (**Figure 2B**). RT-qPCR confirmed the FXR-dependent
175 expression of *FincoR,* similar to that of *Shp* (**Figure 2-Figure Supplement 1B**).
176 We next examined if FXR binds to these enhancers that produce the identified
177 eRNAs by analyzing published mouse liver ChIP-Seq data for FXR (**Supplementary**
178 **Table S3**) *(Thomas et al., 2010; Lee et al., 2012)*. FXR binding was strongly enriched at
179 the enhancers associated with FXR-induced eRNAs as were the enhancer marks
180 H3K27ac and H3K4me1 (**Figure 2-Figure Supplement 1C**). In **Figure 2B**, the results
181 show the binding of FXR and the presence of histone marks at the *FincoR* enhancer
182 region determined by ChIP-seq as compared with nascent transcripts detected by Gro-

183 seq. These analyses support the conclusion that activation of FXR transcriptionally
184 induces this series of eRNAs via chromatin binding at these enhancers, including *FincoR*.
185 We validated FXR binding at the enhancer region that produces *FincoR* using
186 mouse liver ChIP (**Figure 2C**). We also examined binding of a well-known DNA binding
187 partner of FXR, Retinoid x Receptor alpha (RXRα/NR2B1) *(Evans and Mangelsdorf,*
188 *2014; Zheng et al., 2018)*, and bromodomain-containing protein 4 (BRD4), an acetylated
189 histone reader protein that often binds at active enhancers *(Chen et al., 2016; Li et al.,*
190 *2016; Rahnamoun et al., 2018; Sartorelli and Lauberth, 2020)* and a transcriptional
191 coactivator of FXR *(Jung et al., 2020)*. GW4064 treatment resulted in substantial
192 increases in recruitment of both FXR and RXRα to the enhancer region close to the
193 transcription start site of *FincoR* (arrow shown below in Figure 2B), whereas binding was
194 not detected at a control region (**Figure 2C**). We also found that BRD4 occupancy was
195 increased at this enhancer region after GW4064 treatment (**Figure 2C**). These results
196 indicate that GW4064 activation of FXR leads to increased occupancy of the FXR/RXRα
197 heterodimer and BRD4 to the enhancer region to upregulate *FincoR* eRNA in the liver.
198 We identified an inverted repeat1 (IR1) motif that was known to bind FXR *(Lee et*
199 *al., 2006; Calkin and Tontonoz, 2012)* within the major FXR binding peak near the start
200 site of *FincoR* (arrow shown below in Figure 2B), which we also refer to as FXRE (**Figure**
201 **2B, C**). We examined the functionality of this IR1 motif for mediating transcriptional
202 activation by GW4064 using reporter assays (**Figure 2D**). We cloned the region
203 containing the IR1 motif into the pGL4.23 luciferase reporter and generated a mutated
204 IR1 motif construct as a comparison (**Figure 2D**). After transfection into human hepatic
205 HepG2 cells, GW4064 treatment significantly elevated the luciferase activity of the

206 reporter with the wild type IR1 motif, but not with the mutated IR1 motif (**Figure 2D**).
207 Together, these results suggest that GW4064-activated FXR directly upregulates *FincoR*
208 expression.
209
210 ***FincoR* is a liver-specific nucleus-enriched eRNA**
211 Because enhancers and eRNAs generally act in a tissue-specific manner *(Li et al., 2016;*
212 *Sartorelli and Lauberth, 2020)*, we examined the tissue-specific expression of *FincoR* in
213 mice. Strikingly, *FincoR* is highly expressed in the liver and it is expressed at extremely
214 low levels in most other tissues, except for a detectable, but still fairly low, level in the
215 lung. GW4064 treatment resulted in induction of *FincoR* specifically in the liver (**Figure**
216 **3A**). The level of *FincoR* detected in isolated primary mouse hepatocytes (PMHs) was
217 similar to that in mouse liver tissue treated with GW4064, suggesting that the majority of
218 *FincoR* is present in hepatocytes (**Figure 3B**).
219 By using the 5' and 3' rapid amplification of cDNA ends (RACE), we
220 identified one transcript of FincoR that is of approximately 3.7 kb in length (**Figure 3C**).
221 However, based on RNA-seq, the length of *FincoR* is over 10 kb (**Figure 1C**), suggesting
222 there are likely additional multiple RNA isoforms that we were not able to identify by
223 RACE. We next analyzed the coding potential of *FincoR* utilizing a comparative genomic
224 program, PhyloCSF. While adjacent genes *Gcnt1* and *Prune2* (**Figure 3D, E**) were
225 correctly predicted to encode proteins, *FincoR* did not contain a potential protein-coding
226 open reading frame (**Figure 3E**). Consistent with this bioinformatic prediction, a vector
227 expressing *FincoR* failed to produce any proteins in an in vitro transcription/translation
228 assay (**Figure 3F**) confirming that the *FincoR* transcript is a noncoding RNA. *FincoR*

229 transcripts were enriched by binding to oligo-dT beads, suggesting that *FincoR* is 3'
230 polyadenylated (**Figure 3G**). Further, *FincoR* was detected in the nuclear compartment
231 and GW4064 treatment increased the nuclear abundance of *FincoR* (**Figure 3H**),
232 consistent with its potential transcriptional regulatory function. Together, these results
233 from molecular biochemical characterization studies reveal that *FincoR* is a liver-enriched
234 nuclear polyadenylated eRNA.
235

236 ***FincoR* is induced specifically by the hammerhead-type synthetic FXR agonists**

237 To determine whether induction of the FXR-induced FincoR is ligand-specific, we
238 examined the effects of hammerhead-type synthetic FXR agonists, GW4064, cilofexor,
239 and tropifexor; a semi-synthetic agonist, OCA; and a non-hammerhead-type gut-specific
240 agonist, fexaramine (**Figure 4A**) *(Downes et al., 2003; Fang et al., 2015)*. Remarkably,
241 treatment with each of the hammerhead type agonists for 1 h resulted in a robust induction
242 of *FincoR* (**Figure 4B**), whereas *FincoR* levels were unchanged after treatment with OCA
243 or fexaramine for 1 h (**Figure 4B**). Treatment with OCA for 4 h or even one-week
244 treatment with OCA failed to induce hepatic *FincoR* in mice, while expression of *Shp* was
245 significantly induced (**Figure 4C, D**). Acute feeding with a diet supplemented with 0.5%
246 cholic acid (CA), a primary BA, for 6 h also failed to induce *FincoR* expression (**Figure**
247 **4E**). Collectively, these results demonstrate that *FincoR* is induced specifically by
248 hammerhead type FXR agonists.
249

250 **Generation of CRISPR/Cas9-mediated *FincoR* liver-specific knockdown mice**

251 To explore the functional role of hepatic FincoR, we utilized the CRISPR/Cas9 technique
252 to generate FincoR liver-specific knockdown (FincoR-LKD) mice (**Figure 5-Figure**
253 **Supplement 1A**). Adenoviral-mediated sgRNA expression in Cas9 mice resulted in
254 downregulation of FincoR specifically in the liver by about 60%, but not in other tissues
255 (**Figure 5B**). As FXR is a key regulator of bile acid, cholesterol, lipid, and glucose
256 metabolism and FincoR is specifically regulated by FXR, FincoR may have a role in the
257 metabolic process in physiology and disease. We examined liver triglyceride, cholesterol,
258 bile acid, glycogen and serum non-esterified fatty acids (NEFA) but *FincoR*
259 downregulation did not result in any significant changes under physiological conditions
260 (**Figure 5C**).

261 To explore the molecular signatures and pathways affected by FincoR, we
262 examined the global gene expression by RNA-seq analysis in mouse liver after *FincoR*
263 knock-down (**Figure 5D**). While FincoR was markedly downregulated, the neighboring
264 genes, such as *Gcnt1, Rfk, Pcsk5*, were largely unchanged (**Figure 5D**). The RNA-seq
265 analysis revealed 18 up-regulated genes and 53 downregulated genes in FincoR-LKD
266 liver (**Supplementary Table S4; Figure 5E**). GO analysis indicated that these genes
267 were enriched in pathways involved in fatty acid oxidation, organelle organization and
268 metabolic process (**Figure 5F**). Among the down-regulated genes, *Ppp1r3g* which has a
269 role in controlling glycogen synthesis, and *Igfbp2* which functions in insulin resistance,
270 were markedly reduced (**Supplementary Table S4; Figure 5-Figure Supplement 1D,**
271 **E**). Among the up-regulated genes, expression of *Eda2r* was substantially increased,
272 which belongs to a member of tumor necrosis factor receptor superfamily and is involved
273 in inflammation, the immune response and development (**Figure 5-Figure Supplement**

274 **1F**). *Fndc1* which is involved in fibronectin matrix remodeling was also suppressed by
275 FincoR (and thus upregulated upon its KO, **Figure 5-Figure Supplement 1G**). These
276 studies suggested that FincoR may have a role in modulating metabolic homeostasis by
277 regulating genes involved in metabolism and inflammation.
278

279 **Amelioration of hepatic steatosis mediated by tropifexor is independent of FincoR**
280 **in diet-induced NASH mice**

281 Tropifexor, also known as LJN452, is a highly potent hammerhead type FXR agonist that
282 is currently under clinical trials for NASH and PBC patients *(Tully et al., 2017; Kremoser,*
283 *2021; Sanyal et al., 2023)*. Because FincoR is induced specifically by the hammerhead
284 class of FXR agonist (**Figure 4**) and has a potential role in the regulation of metabolism
285 and inflammation (**Figure 5**), we hypothesized that FincoR may play a role in tropifexor-
286 mediated beneficial effects on reducing NASH pathologies in mice.

287 We adopted a mouse model that had been fed the Amylin Liver NASH-promoting
288 (AMLN) diet *(Zhao et al., 2018; Hernandez et al., 2019; Sun et al., 2022)*, and examined
289 the effects of liver-specific downregulation of FincoR in potentially impacting tropifexor
290 effects on NASH pathology. Cas9 mice fed AMLN diet for 12 weeks were injected via tail
291 veins with adenovirus expressing control sgRNA or FincoR sgRNA, respectively, and then
292 treated daily with tropifexor (0.3 mg/kg) for 12 days (**Figure 6A**). In these mice, as a
293 technical validation of RNA induction and knockdown, FincoR levels were significantly
294 increased by FXR agonist tropifexor, and the increase was blocked by adenovirus
295 expressing sgRNA for FincoR (**Figure 6B**).

296 We then examined the effect of tropifexor treatment and FincoR downregulation
297 on hepatic steatosis in these mice. Tropifexor treatment markedly reduced neutral lipids
298 determined by Oil Red O staining of liver sections (**Figure 6C**) and liver TG levels (**Figure**
299 **6D**), and these beneficial effects on reducing fatty liver were not altered by FincoR
300 downregulation. Also, FincoR downregulation had little effects on liver cholesterol and
301 gallbladder bile acid levels, although these levels were reduced by Tropifexor (**Figure 6D**).
302 Consistent with the phenotypes, hepatic expression of key genes involved in BA
303 synthesis was dramatically reduced by tropifexor treatment (i.e., *Cyp7a1 and Cyp8b1*),
304 which is consistent with decreased gallbladder BA levels by this drug (**Figure 6E**).
305 Similarly, tropifexor also lowered lipid synthesis genes (*Srebp1, Lipin*, *Scd1*), consistent
306 with decreased liver TG levels. However, downregulation of *FincoR* did not result in
307 changes in mRNA levels of these genes (**Figure 6E**). These results indicate that
308 tropifexor-mediated beneficial effects on reducing hepatic steatosis are independent of
309 *FincoR*.
310

311 **FincoR facilitates alleviation of liver inflammation by tropifexor in diet-induced**
312 **NASH**

313 Tropifexor ameliorated fibrotic NASH pathologies in preclinical studies *(Tully et al., 2017;*
314 *Hernandez et al., 2019)* and recently completed phase 2 clinical trials for NASH patients
315 *(Sanyal et al., 2023)*. We, therefore, further examined the effects of FincoR
316 downregulation on altering other NASH pathologies, including hepatocellular apoptosis,
317 liver fibrosis and inflammation.

318 In the same AMLN diet-fed mice above (**Figure 6**), analyses of liver sections
319 revealed that tropifexor treatment reduced hepatocyte swelling/ballooning (H&E staining),
320 decreased numbers of apoptotic cells (TUNEL staining), alleviated fibrosis (Sirius red
321 staining), and lowered infiltration of macrophages (F4/80 staining) (**Figure 7A**).
322 Remarkably, these tropifexor-mediated beneficial effects on NASH pathologies were all
323 markedly diminished by FincoR downregulation (**Figure 7A**). This was consistently found
324 in various liver lobes and two representative pictures from 2 different lobes are shown
325 (**Figure 7A**). In control experiments, FincoR downregulation in vehicle-treated mice did
326 not result in marked changes in NASH pathologies (**Figure 7-Figure Supplement 1**).
327 These results demonstrate that FincoR is required for tropifexor-mediated beneficial
328 effects on reducing NASH pathologies, specifically reducing hepatic inflammation, fibrosis
329 and hepatocyte apoptosis. Consistent with these results, serum ALT levels, an indicator
330 of liver damage, were significantly elevated after FincoR downregulation (**Figure 7B**).
331 Protein levels of key inflammatory markers, IL1β and CCL2, in liver extracts were also
332 elevated after FincoR downregulation (**Figure 7C**).
333 Consistent with the phenotypes from histological analyses, hepatic expression of
334 fibrosis and inflammation was altered by FincoR knockdown. For example, tropifexor
335 treatment reduced mRNA levels of several genes that promote fibrosis (*Col1a1, Col1a2,*
336 *Acta2*) and hepatic inflammation (*Eda2r, Ifng, Ccl3)*, whereas these reductions were
337 largely reversed by FincoR downregulation (**Figure 7D**). We also detected increased
338 expression of inflammatory genes (*Ccl2, Ccr2, Lcn2) and* extracellular matrix remodeling
339 gene *(Fndc1)* in mice liver with FincoR knockdown (**Figure 7D**). Tropifexor treatment
340 suppresses hepatic apoptosis by reducing pro-apoptotic genes (*Ctsb, Ctss*) and

341 upregulating anti-apoptotic genes such as *Bcl2 (Warren et al., 2019)*. Importantly, these
342 effects were significantly reversed by FincoR downregulation (**Figure 7D**).
343 Collectively, these results demonstrate that in diet-induced NASH mice,
344 pharmacological activation of FXR by tropifexor reduced fibrosis, apoptosis, and
345 inflammation in NASH mice, which was dependent, at least in part, on the induction of
346 *FincoR*.
347
348 **Discussion**
349 FXR maintains metabolic homeostasis by transcriptional regulation of genes. Direct
350 regulation of protein-coding genes by FXR, including *Shp*, is well characterized. In this
351 study we show that FXR also mediates its functions by induction of lncRNA genes, which
352 vastly outnumber protein-coding genes. We further show that pharmacological activation
353 of FXR by hammerhead-type agonists induces a liver-specific enhancer-derived lncRNA,
354 which we named FincoR, that contributes to reduction of NASH pathologies in mice.
355 FincoR is specifically induced by the hammerhead class of FXR agonists, such as
356 GW4064, cilofexor, and tropifexor. It was not induced by other FXR ligands, including its
357 endogenous ligand, cholic acid, suggesting that FincoR does not contribute to
358 physiological functions of FXR, but instead plays a role in pharmacological FXR
359 responses and possibly in pathological processes. GW4064 is the mother compound of
360 these isoxazole type ligands but is not an ideal therapeutic agent because of its poor
361 water solubility and pharmacokinetics *(Abel et al., 2010)*. In contrast, tropifexor and
362 cilofexor have better pharmacokinetics and were generally well-tolerated in clinical trials
363 for NASH and PBC patients *(Tully et al., 2017; Abenavoli et al., 2018; Kremoser, 2021;*

364 *Sanyal et al., 2023)*, but the underlying mechanisms for their beneficial effects are poorly
365 understood. Intriguingly, a recent study showed that the gene signature regulated by
366 tropifexor-activated FXR appears to be broader than that of OCA, partly because the
367 tropifexor backbone allows a more favorable interaction of FXR with coactivators or
368 epigenomic modulators *(Hernandez et al., 2019)*. Further, tropifexor was shown to
369 regulate distinct sets of genes, particularly those promoting fibrosis, inflammation, and
370 oxidative stress, in experimental NASH *(Hernandez et al., 2019)*. Utilizing CRISPR/Cas9-
371 mediated liver-specific knockdown of FincoR in diet-induced NASH mice, we demonstrate
372 that beneficial effects on reducing liver fibrosis, inflammation, and apoptosis mediated by
373 tropifexor were largely dependent on FincoR (Model, **Figure 7E**).

374 The roles of regulatory RNAs in liver function and diseases and as therapeutic
375 targets or drugs are increasingly being appreciated (*Sallam et al., 2016; Zhao et al., 2018;*
376 *Brocker et al., 2020; Li et al., 2021)*. For example, a critical role for an oxysterol nuclear
377 receptor LXR-induced lncRNA, LeXis, in feedback modulation of cholesterol biosynthesis
378 has been shown *(Sallam et al., 2016)*. Recently, the role of a lncRNA, Pair, in the liver
379 phenylalanine metabolism has been demosntrated *(Li et al., 2021)*. Enhancer RNAs are
380 a less characterized class of lncRNAs and are highly associated with enhancer functions
381 in gene regulation *(Li et al., 2016)*. Numerous studies have revealed transcriptional roles
382 for eRNAs in various cellular processes *(Lai and Shiekhattar, 2014; Lam et al., 2014; Li*
383 *et al., 2016)* but most previous eRNA studies have used culture cells *(Li et al., 2013;*
384 *Hsieh et al., 2014)*, with only a few in vivo studies in mouse models *(Mirtschink et al.,*
385 *2019; Tang et al., 2023)*. In our current study, through integrative analysis of
386 transcriptome and histone mark ChIP-Seq, we identified FXR-induced eRNAs, including

387 the highly induced *FincoR*. We further examined the expression of function of *FincoR*
388 utilizing mouse models. Our current work characterized the role of *FincoR* in gene
389 regulation and in mediating beneficial pharmacological effects of FXR agonists in NASH,
390 representing an important progress in understanding physiological/pathological roles of
391 eRNAs in vivo. Future work is warranted to understand the exact mechanisms by which
392 *FincoR* facilitates action of FXR agonists to alleviate inflammation, fibrosis and apoptosis.
393

394 While this study focused on regulation of *FincoR* by pharmacological activation of
395 FXR, physiological and pathological regulations of *FincoR* appear to be complex. *FincoR*
396 was not induced by acute cholic acid feeding, but *FincoR* levels were elevated in mouse
397 models of cholestatic liver (data not shown), where BA metabolism is dysregulated. Since
398 different BAs can activate or repress the gene-regulating function of FXR *(Wahlstrom et*
399 *al., 2016)*, altered BA composition in cholestatic liver may contribute to induction of
400 *FincoR*. Further, binding peaks for multiple nuclear receptors, FXR, LXR, PPARα, RXRα,
401 and HNF-4α, were detected in the *FincoR* gene locus so that regulation of *FincoR* likely
402 involves combinatorial regulation by multiple nuclear receptors (**Other Supplementary**
403 **Figure 1**). Interestingly, occupancy of the nuclear receptor PPARα at the enhancer region
404 was increased in fasted mice (**Other Supplementary Figure 2**). It will be interesting to
405 see whether expression of *FincoR* is differently regulated by these nuclear receptors in
406 response to physiological and pathological cues.

407 FXR is increasingly recognized as an important therapeutic target for
408 enterohepatic diseases, but the development of clinically applicable and more targeted
409 FXR-based therapy is still challenging. In this study, we provided the first characterization

410 of an eRNA, *FincoR*, induced by pharmacological activation of FXR and show that *FincoR*
411 has a beneficial role in reducing liver fibrosis and inflammation in dietary NASH mice.
412 Complete understanding of the function and mechanisms of *FincoR* may provide novel
413 insights for the development of desirable therapy for NASH and other chronic liver
414 diseases.
415
416

417 **Materials and Methods**

418 **Animal experiments**

419 All animal studies were performed according to procedures approved by the Institutional
420 Animal Care & Use Committee at the University of Illinois at Urbana-Champaign and were
421 in accordance with National Institutes of Health guidelines. Mice were maintained in
422 12/12 h light/dark cycles and fed standard rodent chow. FXR-LKO mice were generated
423 by breeding FXR floxed mice with Albumin-Cre mice (The Jackson Lab). FincoR-LKD
424 mice were generated as previously reported *(Zhao et al., 2018)*. Briefly, Cas9 transgenic
425 mice (JAX #024858) were via the tail vein injected with adenoviruses (approximately
426 $5x10^8$ PFU) expressing two sgRNAs targeting FincoR (sgRNA1:
427 *GGGTTAAGAGCTGTAGGCTG* and sgRNA2: ACTTCTATGTCCAACAACCG). The
428 sequences of sgRNAs were designed using a CRISPR design tool (http://crispr.mit.edu/).

429 Mice were given a single dose of vehicle or 30 mg/kg GW4064 (in corn oil, Tocris
430 Bioscience, #2473) after overnight fasting. Mice were treated with 0.5 mg/kg tropifexor (in
431 corn oil, MedChem Express, HY-107418), 30 mg/kg cilofexor (in corn oil,
432 MedChemExpress, HY-109083), 100 mg/kg fexaramine (in 0.5% methylcellulose,
433 MedChem Express, HY-10912), and 20 mg/kg OCA (in 0.5% methylcellulose, MedChem
434 Express, HY-12222) as indicated. C57BL6 mice were fed with a chow diet containing
435 0.5% CA for 6 hrs *(Jung et al., 2020)*.

436 For liver-specific downregulation of FincoR, mice were fed AMLN diet (Research
437 Diets, D09100310, 40 kcal% fat, 2% cholesterol, 20 kcal% fructose) for 12 weeks and
438 then, were injected with adenovirus expressing control sgRNA or sgRNA targeting FincoR

439 and administration of tropifexor was started 3 days later given at 0.3 mg/kg dissolved in
440 corn oil.
441
442 **RNA-Seq**
443 C57BL/6 mice were fasted overnight and treated with 30 mg/kg GW4064 or vehicle for
444 1 h. RNA-seq was performed as previously described *(Byun et al., 2018; Seok et al., 2018;*
445 *Byun et al., 2020)*. Briefly, the RNAs from livers (n = 2 mice/group, each group contains
446 RNAs pooled from 2 mice) were prepared (RNeasy, Qiagen). Ribosomal RNA was
447 removed with the Ribozero HMR Gold kit (Illumina).
448
449 **Construction of strand-specific RNAseq libraries**
450 Construction of the RNAseq libraries and sequencing on the Illumina NovaSeq 6000 were
451 performed at the Roy J. Carver Biotechnology Center at the University of Illinois at
452 Urbana-Champaign. After DNase digestion, purified total RNAs were analyzed on a
453 Fragment Analyzer (Agilent) to evaluate RNA integrity. The total RNAs were converted
454 into individually barcoded polyadenylated mRNAseq libraries with the Kapa HyperPrep
455 mRNA kit (Roche). Libraries were barcoded with Unique Dual Indexes (UDI's) which have
456 been developed to prevent index switching. The adaptor-ligated double-stranded cDNAs
457 were amplified by PCR for 8 cycles with the Kapa HiFi polymerase (Roche). The final
458 libraries were quantitated with Qubit (ThermoFisher) and the average cDNA fragment
459 sizes were determined on a Fragment Analyzer. The libraries were diluted to 10 nM and
460 further quantitated by qPCR on a CFX Connect Real-Time qPCR system (Bio-Rad) for

461 accurate pooling of barcoded libraries and maximization of number of clusters in the
462 flowcell.
463
464 **Sequencing of libraries in the NovaSeq**
465 The barcoded RNAseq libraries were loaded on one SP lane on a NovaSeq 6000 for
466 cluster formation and sequencing. The libraries were sequenced from one end of the
467 fragments for a total of 100 bp. The fastq read files were generated and demultiplexed
468 with the bcl2fastq v2.20 Conversion Software (Illumina, San Diego, CA). The quality of
469 the demultiplexed fastq files was evaluated with the FastQC software, which generates
470 reports with the quality scores, base composition, k-mer, GC and N contents, sequence
471 duplication levels and overrepresented sequences.
472
473 **GRO-seq**
474 To harvest the nuclei from mouse liver cells, the liver was harvested at indicated time and
475 washed with a cold swelling buffer (10 mM Tris pH 7.5, 2 mM $MgCl_2$, 3 mM $CaCl_2$, 2 U/ml
476 Superase-In). The nuclei were prepared by Dounce homogenization in cold swelling
477 buffer and filtered using the cell strainer (100 μm, BD Biosciences). Nuclei were collected
478 by centrifugation at 400 x g for 10 min, then resuspended in the lysis buffer (swelling
479 buffer with 10% glycerol and 1% IGEPAL) and incubated on ice for 5 min. Nuclei were
480 washed twice with the lysis buffer and resuspended at a concentration of $10^8$ nuclei/ml in
481 the freezing buffer (50 mM Tris pH 8.3, 40% glycerol, 5 mM $MgCl_2$, 0.1 mM EDTA). We
482 then followed our previous method *(Li et al., 2013; Oh et al., 2021)* to conduct nuclear
483 run-on and GRO-Seq library preparation. Briefly, the nuclei in freezing buffer were

484 subjected to the nuclear run-on reaction by mixing with an equal volume of run-on buffer
485 (10 mM Tris-Cl pH 8.0, 5 mM $MgCl_2$, 1 mM dithiothreitol (DTT), 300 mM KCl, 20 units of
486 Superase-In, 1% sarkosyl, 500 μM ATP, GTP, Br-UTP and 2 μM CTP) for 5 min at 30 °C.
487 The BrU-labeled run-on RNAs were extracted by TRIzol and purified by anti-BrdU
488 agarose beads (Santa Cruz Biotech, sc-32323 AC). The run-on RNAs were then
489 subjected to end repair by T4 PNK, poly-adenylation, and then to cDNA first strand
490 synthesis by a custom primer (oNTI223) that allows circularization of the cDNA. This
491 cDNA then was re-linearized by Ape1 (NEB), size selected by TBE gel and the products
492 of the desired size were excised (~320–350 bp) for final library prep and sequencing.
493 GRO-Seq samples were run on a NextSeq 500 sequencer from Illumina with a single-
494 end 80 nt model.
495
496 **Histological analyses**
497 For histology, tissues were dissected and immediately fixed in 10% formalin overnight
498 and processed for paraffin embedding and H&E staining. Paraffin-embedded liver
499 sections were incubated with F4/80 antibody, and antibody was detected using a
500 peroxidase-based method (Abcam, ab64238). Liver collagen was detected by Sirius Red
501 staining (Abcam, ab246832) and apoptosis was detected by TUNEL staining (Millipore,
502 S7100). For Oil Red O staining, liver tissue was frozen in OCT compound (Sakura
503 Finetek, 4583), sectioned, and stained. Liver sections were imaged with a NanoZoomer
504 Scanner (Hamamatsu) and quantification was done using NIH ImageJ.
505
506 **Metabolic analyses**

507 Hepatic levels of TG (Sigma, MAK266), cholesterol (Sigma, MAK043), glycogen
508 (Biovision, K646-100), total BA levels (Diazyme, DZ042A), serum NEFA (Sigma,
509 MAK044) and serum ALT (Sigma, MAK052) were determined according to the
510 manufacturer's instructions. Mouse liver IL-1β (R&D systems, MLB00C) and CCL2 (R&D
511 systems, DY479-05) were detected by commercially available ELISA kit.
512
513 **Mouse liver ChIP**
514 Liver ChIP assay was performed as described previously *(Seok et al., 2018; Byun et al.,*
515 *2020; Jung et al., 2020)*. Briefly, chromatin extracts were prepared from FXR floxed and
516 FXR-LKO mouse livers after treatment of the mice with GW4064 which was followed by
517 preclearing and immunoprecipitation using control IgG or FXR antibody (Novus
518 Biologicals, NBP2-16550; Santa Cruz, sc-25309), RXRα antibody (Proteintech, catalog
519 no. 21218-1-AP), or BRD4 antibody (Bethyl Laboratories, catalog #A301-985A50).
520 Enrichment in chromatin precipitates of gene sequences was measured by qRCR using
521 primers listed (**Supplementary Table S5**).
522
523 **Primary mouse hepatocytes and HepG2 cells**
524 Primary hepatocytes were isolated from C57BL/6 mice by collagenase (Worthington
525 Biochemical Corporation, LS004188) perfusion and maintained in William's E Medium
526 with primary hepatocyte maintenance supplements (Gibco #CM4000) in six-well plates
527 as described previously *(Kim et al., 2015; Jung et al., 2020)*. HepG2 cells were maintained
528 in DMEM supplemented with 10% fetal bovine serum at 37°C and 5% $CO_2$.
529

530 **Luciferase reporter assay**

531 The enhancer region containing the FXR binding element was amplified by PCR and
532 cloned into the pGL4.23 vector (Promega). HepG2 cells were transiently transfected with
533 FXR (100 ng/well) and RXRα (5 ng/well) in combination with reporters containing the wild
534 type FXRE or mutated FXRE (200 ng/well) (**Supplementary Table S5**). β-galactosidase
535 plasmid (200 ng/well) was also transfected as internal controls. Cells were treated with
536 GW4064 or DMSO after transient transfection. Six hours later, the cells were harvested.
537 All reporter assays were repeated at least three times in triplicates.

538

539 **RACE**

540 5' and 3' RACE assays were performed using a SMARTer RACE kit (Clontech) according
541 to the manufacturer's instructions. The resulting PCR products were separated by
542 electrophoresis in agarose gels and cloned into the pRACE vector provided by the kit.
543 The transcription start sites and end sites of FincoR were determined by sequencing. The
544 gene-specific primers used for 5'- and 3'-RACE are provided (**Supplementary Table S5**).

545

546 **In vitro transcription and translation (TNT)**

547 Expression plasmids for luciferase and FincoR were mixed with a Coupled Reticulocyte
548 Lysate System (Promega). After incubating at 30ºC for 60 min, translated products were
549 separated on 4-20% gradient SDS polyacrylamide gels and transferred to PVDF
550 membranes. Chemiluminescent detection of in vitro translated protein was performed
551 following the manufacturer's protocol (Promega).

552

553 **RT-qPCR**

554 Total RNA was extracted using RNeasy Mini Kit (Qiagen, 74104) and 2 μg of RNA was
555 reverse transcribed and relative mRNA expression was normalized to those of 36B4. The
556 qPCR primers are shown in **Supplementary Tables S5**.

557

558 **Subcellular fractionation**

559 Using a Cytoplasmic and Nuclear RNA Purification Kit (Norgen, Thorold, ON, Canada),
560 the cytoplasm and nucleus fractions from primary hepatocytes isolated from livers of mice
561 treated with GW4064 or DMSO were separated, and both fractions were subjected to
562 RNA extraction and qRT-PCR.

563

564 **Immunoblotting analysis**

565 Total liver lysates were prepared as described before *(Sun et al., 2022)*. Antibodies for
566 immunoblotting for $\beta$-ACTIN (#4970) were purchased from Cell Signaling Technology.
567 Antibodies for immunoblotting for FXR (sc-25309) were purchased from Santa Cruz.

568

569 **FincoR polyadenylation study**

570 Total RNA was prepared using the RNeasy mini prep kit (Qiagen). Poly(A)+ and poly(A)-
571 RNA was separated by Dynabeads™ mRNA Purification Kit (ThermoFisher Scientific)
572 according to the manufacturer's instructions. Briefly, total RNA was incubated with the
573 Dynabeads/binding buffer suspension at room temperature for 5 min and the reaction
574 tubes were placed on a magnet until solution was clear. The supernatant containing
575 poly(A)- RNA was saved. The beads with poly(A)+ RNA were washed three times with
576 washing buffer provided by the kit. RNA was extracted from the supernatant and beads

577 respectively using Trizol. qPCR was performed to analyze levels of FincoR and 36b4 in
578 the Poly(A)+ and poly(A)- RNA fractions.
579
580 **Genomics Analysis**
581 RNA-Seq and GRO-Seq reads were mapped to the mouse reference genome mm10 with
582 STAR aligner. Transcript quantifications were done with HOMER tool set and enhancer
583 RNAs were identified based on H3K27ac ChIP-Seq in mouse liver. Briefly, intergenic
584 H3K27ac ChIP-Seq peaks were selected as putative enhancer regions in mouse liver.
585 Then +/- 3kb regions around putative enhancers with RNA-Seq signal (>1 RPKM) were
586 considered as putative eRNAs in mouse livers. Overlapped eRNAs regions were merged,
587 and redundant ones were removed. In addition, any +/- 3kb extended eRNAs regions that
588 overlapped with protein-coding genes were further removed to avoid transcriptional
589 readthrough from genes. We used DESeq2 to identify significantly regulated eRNAs with
590 a cutoff of (FDR < 0.05, Log2FC > 1). Public ChIP-Seq datasets were obtained from
591 ENCODE or GEO (**Supplementary Table S3**).
592
593 **Statistical analysis**
594 Statistical analysis was performed using GraphPad Prism 9. Statistical differences were
595 evaluated using two-tailed unpaired Student's t-test for comparisons between two groups,
596 or ANOVA and appropriate post hoc analyses for comparisons of more than two groups.
597 Statistical methods and corresponding *p* values for data shown in each panel were
598 indicated in figure legends.
599

600 **Data availability**

601 RNA-seq and Gro-seq data were deposited in GEO under the following accession
602 numbers GSE 221986.

603

604 **Acknowledgments**

605 We thank Deepa Prakashini Govindasamy Rajagopal for the help with tissue genotyping.
606 We also thank Kristina Schoonjans at Ecole Polytech, Switzerland, for providing FXR
607 floxed mice. This study was supported by an American Diabetes Association Postdoctoral
608 Fellowship to J.C. (1-19-PDF-117), and by a John and Rebekah Harper Fellowship to
609 R.W. W.L. is a Cancer Prevention and Research Institute of Texas (CPRIT) Scholar. This
610 work is supported by funding from NCI (K22CA204468), NIGMS (R21GM132778,
611 R01GM136922), Welch Foundation (AU-2000-20220331), CPRIT (RR160083) to W.L.,
612 and grants from the NIH (R01 DK062777 and R01 DK095842) to J.K.K.

613

614 **References**

615 Abel U, Schluter T, Schulz A, et al. 2010. Synthesis and pharmacological validation of a
616 novel series of non-steroidal FXR agonists. *Bioorg Med Chem Lett* **20**: 4911-
617 4917.

618 Abenavoli L, Falalyeyeva T, Boccuto L, et al. 2018. Obeticholic Acid: A New Era in the
619 Treatment of Nonalcoholic Fatty Liver Disease. *Pharmaceuticals (Basel)* **11**.

620 Ali AH, Carey EJ, Lindor KD. 2015. Recent advances in the development of farnesoid X
621 receptor agonists. *Ann Transl Med* **3**: 5.

622 Brocker CN, Kim D, Melia T, et al. 2020. Long non-coding RNA Gm15441 attenuates
623 hepatic inflammasome activation in response to PPARA agonism and fasting.
624 *Nat Commun* **11**: 5847.

625 Byun S, Kim DH, Ryerson D, et al. 2018. Postprandial FGF19-induced phosphorylation
626 by Src is critical for FXR function in bile acid homeostasis. *Nat Commun* **9**: 2590.

627 Byun S, Seok S, Kim YC, et al. 2020. Fasting-induced FGF21 signaling activates
628 hepatic autophagy and lipid degradation via JMJD3 histone demethylase. *Nat*
629 *Commun* **11**: 807.

630 Calkin AC, Tontonoz P. 2012. Transcriptional integration of metabolism by the nuclear
631 sterol-activated receptors LXR and FXR. *Nat Rev Mol Cell Biol* **13**: 213-224.

632 Cech TR, Steitz JA. 2014. The noncoding RNA revolution-trashing old rules to forge
633 new ones. *Cell* **157**: 77-94.

634 Chen J, Wang Z, Hu X, et al. 2016. BET Inhibition Attenuates Helicobacter pylori-
635 Induced Inflammatory Response by Suppressing Inflammatory Gene
636 Transcription and Enhancer Activation. *J Immunol* **196**: 4132-4142.

637 Claudel T, Staels B, Kuipers F. 2005. The Farnesoid X receptor: a molecular link
638 between bile acid and lipid and glucose metabolism. *Arterioscler Thromb Vasc*
639 *Biol* **25**: 2020-2030.
640 Consortium EP. 2012. An integrated encyclopedia of DNA elements in the human
641 genome. *Nature* **489**: 57-74.
642 Downes M, Verdecia MA, Roecker AJ, et al. 2003. A chemical, genetic, and structural
643 analysis of the nuclear bile acid receptor FXR. *Mol Cell* **11**: 1079-1092.
644 Evans RM, Mangelsdorf DJ. 2014. Nuclear Receptors, RXR, and the Big Bang. *Cell*
645 **157**: 255-266.
646 Fang B, Everett LJ, Jager J, et al. 2014. Circadian enhancers coordinate multiple
647 phases of rhythmic gene transcription in vivo. *Cell* **159**: 1140-1152.
648 Fang S, Suh JM, Reilly SM, et al. 2015. Intestinal FXR agonism promotes adipose
649 tissue browning and reduces obesity and insulin resistance. *Nat Med* **21**: 159-
650 165.
651 Friedman SL, Neuschwander-Tetri BA, Rinella M, et al. 2018. Mechanisms of NAFLD
652 development and therapeutic strategies. *Nat Med* **24**: 908-922.
653 Goodwin B, Jones SA, Price RR, et al. 2000. A regulatory cascade of the nuclear
654 receptors FXR, SHP-1, and LRH-1 represses bile acid biosynthesis. *Mol Cell* **6**:
655 517-526.
656 Hernandez ED, Zheng L, Kim Y, et al. 2019. Tropifexor-Mediated Abrogation of
657 Steatohepatitis and Fibrosis Is Associated With the Antioxidative Gene
658 Expression Profile in Rodents. *Hepatol Commun* **3**: 1085-1097.
659 Hirabayashi S, Bhagat S, Matsuki Y, et al. 2019. NET-CAGE characterizes the

660 dynamics and topology of human transcribed cis-regulatory elements. *Nat Genet*
661 **51**: 1369-1379.
662 Hon CC, Ramilowski JA, Harshbarger J, et al. 2017. An atlas of human long non-coding
663 RNAs with accurate 5' ends. *Nature* **543**: 199-204.
664 Hsieh CL, Fei T, Chen Y, et al. 2014. Enhancer RNAs participate in androgen receptor-
665 driven looping that selectively enhances gene activation. *Proc Natl Acad Sci U S*
666 *A* **111**: 7319-7324.
667 Jung H, Chen J, Hu X, et al. 2020. BRD4 inhibition and FXR activation, individually
668 beneficial in cholestasis, are antagonistic in combination. *JCI Insight* **6**.
669 Kim YC, Fang S, Byun S, et al. 2015. Farnesoid X receptor-induced lysine-specific
670 histone demethylase reduces hepatic bile acid levels and protects the liver
671 against bile acid toxicity. *Hepatology* **62**: 220-231.
672 Kliewer SA, Mangelsdorf DJ. 2015. Bile Acids as Hormones: The FXR-FGF15/19
673 Pathway. *Dig Dis* **33**: 327-331.
674 Kremoser C. 2021. FXR agonists for NASH: How are they different and what difference
675 do they make? *J Hepatol* **75**: 12-15.
676 Lai F, Shiekhattar R. 2014. Enhancer RNAs: the new molecules of transcription. *Curr*
677 *Opin Genet Dev* **25**: 38-42.
678 Lam MT, Li W, Rosenfeld MG, et al. 2014. Enhancer RNAs and regulated
679 transcriptional programs. *Trends Biochem Sci* **39**: 170-182.
680 Lee FY, Lee H, Hubbert ML, et al. 2006. FXR, a multipurpose nuclear receptor. *Trends*
681 *Biochem Sci* **31**: 572-580.
682 Lee J, Padhye A, Sharma A, et al. 2010. A pathway involving farnesoid X receptor and

683 small heterodimer partner positively regulates hepatic sirtuin 1 levels via
684 microRNA-34a inhibition. *J Biol Chem* **285**: 12604-12611.
685 Lee J, Seok S, Yu P, et al. 2012. Genomic analysis of hepatic farnesoid X receptor
686 binding sites reveals altered binding in obesity and direct gene repression by
687 farnesoid X receptor in mice. *Hepatology* **56**: 108-117.
688 Lee JM, Wagner M, Xiao R, et al. 2014. Nutrient-sensing nuclear receptors coordinate
689 autophagy. *Nature* **516**: 112-115.
690 Li W, Notani D, Ma Q, et al. 2013. Functional roles of enhancer RNAs for oestrogen-
691 dependent transcriptional activation. *Nature* **498**: 516-520.
692 Li W, Notani D, Rosenfeld MG. 2016. Enhancers as non-coding RNA transcription units:
693 recent insights and future perspectives. *Nat Rev Genet* **17**: 207-223.
694 Li Y, Tan Z, Zhang Y, et al. 2021. A noncoding RNA modulator potentiates
695 phenylalanine metabolism in mice. *Science* **373**: 662-673.
696 Mattick JS, Amaral PP, Carninci P, et al. 2023. Long non-coding RNAs: definitions,
697 functions, challenges and recommendations. *Nat Rev Mol Cell Biol* **24**: 430-447.
698 Mirtschink P, Bischof C, Pham MD, et al. 2019. Inhibition of the Hypoxia-Inducible
699 Factor 1alpha-Induced Cardiospecific HERNA1 Enhance-Templated RNA
700 Protects From Heart Disease. *Circulation* **139**: 2778-2792.
701 Oh S, Shao J, Mitra J, et al. 2021. Enhancer release and retargeting activates disease-
702 susceptibility genes. *Nature* **595**: 735-740.
703 Rahnamoun H, Lee J, Sun Z, et al. 2018. RNAs interact with BRD4 to promote
704 enhanced chromatin engagement and transcription activation. *Nat Struct Mol Biol*
705 **25**: 687-697.

706 Sallam T, Jones MC, Gilliland T, et al. 2016. Feedback modulation of cholesterol
707 metabolism by the lipid-responsive non-coding RNA LeXis. *Nature* **534**: 124-128.
708 Sanyal AJ, Lopez P, Lawitz EJ, et al. 2023. Tropifexor for nonalcoholic steatohepatitis:
709 an adaptive, randomized, placebo-controlled phase 2a/b trial. *Nat Med* **29**: 392-
710 400.
711 Sartorelli V, Lauberth SM. 2020. Enhancer RNAs are an important regulatory layer of
712 the epigenome. *Nat Struct Mol Biol* **27**: 521-528.
713 Seok S, Fu T, Choi SE, et al. 2014. Transcriptional regulation of autophagy by an FXR-
714 CREB axis. *Nature* **516**: 108-111.
715 Seok S, Kim YC, Byun S, et al. 2018. Fasting-induced JMJD3 histone demethylase
716 epigenetically activates mitochondrial fatty acid beta-oxidation. *J Clin Invest* **128**:
717 3144-3159.
718 Seok S, Sun H, Kim YC, et al. 2021. Defective FXR-SHP Regulation in Obesity
719 Aberrantly Increases miR-802 Expression, Promoting Insulin Resistance and
720 Fatty Liver. *Diabetes* **70**: 733-744.
721 Statello L, Guo CJ, Chen LL, et al. 2021. Gene regulation by long non-coding RNAs and
722 its biological functions. *Nat Rev Mol Cell Biol* **22**: 96-118.
723 Sun H, Seok S, Jung H, et al. 2022. Obesity-induced miR-802 directly targets AMPK
724 and promotes nonalcoholic steatohepatitis in mice. *Mol Metab* **66**: 101603.
725 Tang X, Luo Y, Yuan D, et al. 2023. Long noncoding RNA LEENE promotes
726 angiogenesis and ischemic recovery in diabetes models. *J Clin Invest* **133**.
727 Thomas AM, Hart SN, Kong B, et al. 2010. Genome-wide tissue-specific farnesoid X
728 receptor binding in mouse liver and intestine. *Hepatology* **51**: 1410-1419.

729 Tully DC, Rucker PV, Chianelli D, et al. 2017. Discovery of Tropifexor (LJN452), a
730 Highly Potent Non-bile Acid FXR Agonist for the Treatment of Cholestatic Liver
731 Diseases and Nonalcoholic Steatohepatitis (NASH). *J Med Chem* **60**: 9960-9973.
732 Wahlstrom A, Sayin SI, Marschall HU, et al. 2016. Intestinal Crosstalk between Bile
733 Acids and Microbiota and Its Impact on Host Metabolism. *Cell Metab* **24**: 41-50.
734 Wang YD, Chen WD, Wang M, et al. 2008. Farnesoid X receptor antagonizes nuclear
735 factor kappaB in hepatic inflammatory response. *Hepatology* **48**: 1632-1643.
736 Warren CFA, Wong-Brown MW, Bowden NA. 2019. BCL-2 family isoforms in apoptosis
737 and cancer. *Cell Death Dis* **10**: 177.
738 Zhao XY, Xiong X, Liu T, et al. 2018. Long noncoding RNA licensing of obesity-linked
739 hepatic lipogenesis and NAFLD pathogenesis. *Nat Commun* **9**: 2986.
740 Zheng W, Lu Y, Tian S, et al. 2018. Structural insights into the heterodimeric complex of
741 the nuclear receptors FXR and RXR. *J Biol Chem* **293**: 12535-12541.

742

743
744

745 **Figure legends**

746 **Figure 1. Activation of FXR by GW4064 induces *FincoR*, a novel eRNA, in mouse**
747 **liver.** (A) C57BL/6 male mice were fasted overnight and *i.p.* injected with vehicle or
748 GW4064 (30 mg/kg) for 1 h, and livers were collected (n = 4 mice). RNAs from two mice
749 (per group) were pooled for RNA-seq. Volcano plot showing significantly induced eRNAs
750 (FincoR highlighed) by GW4064 treatment. The *x* axis denotes $\log_2$ fold change
751 (GW4064/Veh) of eRNAs and the *y* axis denotes $-\log_{10}$ FDR of eRNAs. (B) The bar plot
752 showing the RPMs of up-regulated eRNAs by GW4064 treatment. (C) FincoR induction
753 by GW4064 treatment was shown in the genome browser track. (D) GW4064 induction
754 of *FincoR* and *Shp* was measured in the liver by qPCR (n = 4 mice). Data are presented
755 as mean ± SEM. Statistical significance was determined by the two-way ANOVA Sidak's
756 multiple comparisons test with $*p < 0.05$ and $***p < 0.001$. Veh, vehicle; GW, GW4064;
757 pos, positive strand; neg, negative strand; Refseq, reference sequence.

758 **Figure 2. Ligand-activated FXR directly activates transcription of eRNAs including**
759 ***FincoR* in the liver.** (A) Experimental outline: FXR-Flox and LKO male mice were fasted
760 overnight and treated with vehicle or GW4064, livers were collected 1 h later (n = 2 each)
761 and nuclei was isolated for Gro-seq. Box plot shows the up-regulated eRNA GRO-Seq
762 RPKMs in different conditions. (B) Gro-seq profile of *FincoR* expression and genome
763 browser tracks of H3K4me1, H3K27ac, FXR and RXRα binding peaks at *FincoR* locus
764 were shown. (C) ChIP assays were performed in liver samples from Fig. 1A to detect
765 FXR, RXRα, and BRD4 occupancy to the FXR binding peak region close to the
766 transcription start site of *FincoR*. (D) HepG2 cells were transfected with luciferase reporter

767 expressing wild type FXRE or mutant FXRE (see materials and methods) for 24 hrs before
768 further subject to GW4064 for 6 hrs. The relative luciferase activity was shown.

769 **Figure 3. *FincoR* is a liver-specific nucleus-enriched eRNA.** (A) C57BL/6 male mice
770 were fasted overnight and *i.p.* injected with vehicle or GW4064 (30 mg/kg) for 1 h. Tissues
771 were collected and *FincoR* mRNA level was measured (n = 2 mice). (B) C57BL/6 male
772 mice were fasted overnight and *i.p.* injected with vehicle or GW4064 (30 mg/kg) for 1 h.
773 One small piece of liver was snap-frozen for later RNA isolation and the remaining part
774 was used for immediate primary hepatocyte isolation. Then, RNAs were extracted from
775 liver or primary hepatocytes and *FincoR* expression was measured. (C) Agarose gel
776 electrophoresis of PCR products generated in 5′ (left) and 3′ (right) RACE of *FincoR* in
777 liver samples. Primer locations were show. (D) Schematic diagrams of full-length *FincoR*.
778 (E) PhyloCSF analysis of the coding potential of *FincoR*. (F) In vitro translation of *FincoR*
779 using the Promega Transcend Non-Radioactive Translation Detection Systems.
780 Luciferase is used as controls for coding RNA. (G) qPCR analysis of *FincoR*, *36b4* in
781 Poly(A)+ and Poly(A)- RNA fractions from GW4064 treated mouse liver. (H) *FincoR*
782 identified in the subcellular fraction using cellular fractionation assays. The primary
783 hepatocytes were isolated from GW4064 or DMSO treated mouse liver and the cytoplasm
784 and nucleus fractions of these hepatocytes were separated and both fractions were
785 subjected to RNA extraction and qPCR. RACE, rapid amplification of cDNA ends.

786 **Figure 4. FincoR is induced by the hammerhead class of non-steroidal FXR**
787 **agonists, including GW4064 and tropifexor.** (A) The chemical structures of the FXR
788 agonists including the hammerhead class of non-synthetic FXR agonists, non-
789 hammerhead-type non-synthetic agonists, semi-synthetic BA and natural BA. (B)

790 C57BL/6 mice were treated with GW4064 (30 mg/kg) or Cilofexor (30 mg/kg) or Tropifexor
791 (0.5 mg/kg) or Fexaramine (100 mg/kg) or OCA (20 mg/kg) for 1 h after over-night fasting.
792 The liver RNAs were extracted and FincoR expression was measured (n = 3~4 mice). (C)
793 C57BL/6 mice were treated with OCA (20 mg/kg) or Fexaramine (100 mg/kg) for 4 hrs
794 after over-night fasting. The liver RNAs were extracted and FincoR expression was
795 measured (n = 3 mice). (D) C57BL/6 mice were daily treated with OCA (20 mg/kg) for 7
796 days after over-night fasting. The liver RNAs were extracted and FincoR expression was
797 measured (n = 5 mice). *Shp* gene was used as a positive control. (E) C57BL/6 mice were
798 fed with 0.5% cholic acid (CA) diet for 6 hrs after over-night fasting. The liver RNAs were
799 extracted and FincoR expression was measured (n = 3~4 mice). (B-E) Data are presented
800 as mean ± SEM. Statistical significance was determined by the Student's t test with *$p$ <
801 0.05, **$p$ < 0.01 and ***$p$ < 0.001.

802 **Figure 5. Generation of CRISPR/Cas9-mediated *FincoR* liver-specific knockdown**
803 **mice.** (A) Male Cas9 mice were infected with adenovirus expressing sgRNA for *FincoR*
804 or control for 1 week. Then the liver and serum were collected from these mice after 4~5
805 hrs of fasting. (B) The expression of FincoR in the liver was measured by qPCR (n = 4
806 mice). (C) Hepatic triglyceride, cholesterol, bile acid, glycogen and serum NEFA were
807 measured (n = 5~7 mice) (D) Male Cas9 mice were infected with adenovirus expressing
808 sgRNA for *FincoR* or control for 1 week. Then these mice were fasted overnight and
809 treated with GW4064 for 3 hrs before tissue collection. RNA-seq profiles of expression of
810 hepatic *FincoR* and the adjacent genes were shown (n = 2 mice). (E) Genome-wide
811 changes in mRNA expression shown in a volcano plot. The numbers refer to the number

812 of genes up- or down-regulated by 2-fold or more with a *p*-value < 0.01. (F) Gene ontology
813 analysis of biological pathways using DAVID Tools.

814 **Figure 6. In diet-induced NASH mice, tropifexor-mediated beneficial effects on**
815 **reducing hepatic steatosis are largely independent on FincoR.** (A-E) Male Cas9 mice
816 were fed with NASH diet for 12 weeks. Then these mice were randomly assigned to 3
817 groups and infected with adenovirus expressing sgRNA for *FincoR* or control. Three days
818 later, the mice were treated with Tropifexor (0.3 mg/kg) for 12 days. On the tissue
819 collection day, the mice were given the last shot of Tropifexor or vehicle and fasted for 4
820 hrs before tissues were collected (n = 6 ~ 7 mice). (A) Experimental scheme. (B) Hepatic
821 FincoR expression was measured (n = 6~7 mice). (C) Oil Red O staining of liver sections.
822 Scale bar (50 μm). (D) Hepatic TG, hepatic cholesterol, gallbladder BA and hepatic BA
823 levels were measured (n = 6 ~ 7 mice). (E) mRNA levels in the liver of the indicated genes
824 involved in bile acid regulation and lipid regulation (n = 6 ~ 7 mice). (B, D and E) Data are
825 presented as mean ± SEM. Statistical significance was determined by the one-way
826 ANOVA (Sidak's multiple comparisons test) with *$p < 0.05$, **$p < 0.01$ and ***$p < 0.001$.
827 Ad, adenovirus; H & E, hematoxylin and eosin; TG, triglyceride; Veh, vehicle; ns, not
828 significant.

829 **Figure 7. In diet-induced NASH mice, tropifexor-mediated beneficial effects on**
830 **reducing liver fibrosis and inflammation are diminished by FincoR downregulation.**
831 (A) H & E, F4/80, Sirius Red and TUNEL staining of liver sections from Figure 6. Scale
832 bar (50 μm). Image analyses were done using Image J and the area of collagen staining,
833 TUNEL and F4/80 levels were quantified (n = 5/group). (B) Serum ALT level was
834 measured (n = 5/group). (C) IL-1β and CCL2 levels in the liver tissues were determined

835 by ELISA (n = 5/group). (D) mRNA levels in the liver of the indicated genes involved in
836 inflammation, fibrosis and cell death (n = 5/group). (E) Model: FincoR is a liver-specific
837 lncRNA that is induced specifically by hammerhead-type FXR agonists (top). In diet-
838 induced NASH mice, *FincoR* is required for tropifexor-mediated beneficial effects on
839 reducing hepatic inflammation, fibrosis, and cell death with the mechanisms to be
840 explored further (bottom). (A-D) Data are presented as mean ± SEM. Statistical
841 significance was determined by the one-way ANOVA (Sidak's multiple comparisons test)
842 with *$p < 0.05$, **$p < 0.01$ and ***$p < 0.001$.
843
844

845 **Supplementary Figure Legends**

846 **Figure 1- Figure Supplement 1.** (A, B) Examples of FXR-regulated eRNAs produced
847 near the genes *Hes1* (A) and *Slc35g1* (B) were shown. (C) Time course expression of
848 *FincoR*. C57BL/6 male mice were fasted overnight and *i.p.* injected with vehicle or
849 GW4064 (30 mg/kg) for 1, 3, 6,12 h. Livers were collected at indicated time points (n = 3
850 mice) and *FincoR*, *Shp* and *Gcnt1* were measured. Data are presented as mean ± SEM.
851 Statistical significance was determined by the two-way ANOVA Sidak's multiple
852 comparisons test with $*p < 0.05$ and $***p < 0.001$.

853 **Figure 1- Figure Supplement 2.** (A) Volcano plot showing the differential expressed
854 genes (DEGs) by GW4064 treatment (DESeq2 FDR<0.05). The numbers refer to the
855 number of genes up- or down-regulated. (B) Bar plot showing the enriched Gene ontology
856 in terms of biological processes for up-regulated genes.

857 **Figure 2- Figure Supplement 1**. (A) FXR protein levels in the livers isolated from FXR-
858 Flox and FXR-LKO mice were shown. (B) Validation of hepatic FXR-dependent induction
859 of *FincoR* by qPCR (n = 3 mice). *Shp* gene was used as a control. Data are presented as
860 mean ± SEM. Statistical significance was determined by the two-way ANOVA Tukey's
861 multiple comparisons test with $*p < 0.05$, $**p < 0.01$ and $***p < 0.001$. (C) Metagene plots
862 showing H3K27ac, H3K4me1, FXR, and RXRα ChIP-Seq profiles centered on up-
863 regulated eRNAs.

864 **Figure 5- Figure Supplement 1**. (A) The scheme for the *FincoR* loss of function
865 experiments. (B) The genomic DNAs from liver, spleen, intestine, brain, heart, muscle,
866 kidney, lung and adipose tissue were isolated and PCR was performed using the primers
867 (**Supplementary Table S5E**) to verify tissue-specific knock-out. (C-G) RNA-seq profiles

868 of expression of hepatic *Prune2* (C)*, PPP1r3g* (D)*, Igfbp2* (E)*, Eda2r* (F) *and Fndc1* (G)
869 were shown (n = 2 mice).

870 **Figure 7- Figure Supplement 1. The effects of FincoR downregulation on NASH**
871 **pathologies.** Male Cas9 mice were fed with NASH diet for 12 weeks. Then these mice
872 were randomly assigned to 2 groups and infected with adenovirus expressing sgRNA for
873 *FincoR* or control. The tissues were collected 2 weeks later. Liver histology analysis was
874 performed. Scale bar (50 μm).

875 **Other Supplementary Figure 1. Hepatic genome browser tracks of FXR, RXRα, LXR,**
876 **PPARα, and HNF4α binding peaks at *FincoR* locus.**

877 **Other Supplementary Figure 2. PPARα occupnacy in the FincoR enhancer region.**
878 C57BL/6 male mice were fasted overnight with or without refed for 3 hrs and then
879 sacrificed. ChIP assays were performed in liver samples to detect PPARα occupancy to
880 the FXR binding peak region close to the transcription start site of *FincoR*.

881
882
883
884
885

886 **Supplemental Tables**

887

888 Supplemental Table S1. Sequencing data generated in this study

| Name | Total reads | Uniquely mapped reads |
|---|---|---|
| WT Liver Veh RNA-Seq rep1 | 50887391 | 38072659 |
| WT Liver GW RNA-Seq rep1 | 54020150 | 40595856 |
| WT Liver Veh RNA-Seq rep2 | 51268164 | 38898913 |
| WT Liver GW RNA-Seq rep2 | 51899892 | 39487241 |
| Flox Liver Veh GRO-Seq | 62960996 | 30305910 |
| Flox Liver GW GRO-Seq | 59210073 | 26116795 |
| FXR KO Liver Veh GRO-Seq | 34153537 | 14379417 |
| FXR KO Liver GW GRO-Seq | 36430101 | 15008281 |
| WT Liver RNA-Seq rep1 | 96262381 | 81801494 |
| WT Liver RNA-Seq rep2 | 104979915 | 88365481 |
| FincoR KD Liver RNA-Seq rep1 | 91654076 | 75346167 |
| FincoR KD Liver RNA-Seq rep2 | 90211420 | 74745807 |

889

890 Supplemental Table S2 is attached as an Excel file.

891

892 Supplemental Table S3. Public ChIP-Seq dataset

| target | accession ID |
|---|---|
| FXR | https://genome.ucsc.edu/cgi-bin/hgCustom?hgsid=1577671033_RPWVA7jbx3rDswKOeo2dazTsXxe0&hgct_table=ct_FxrLiver_2971 |
| H3K27ac | ENCFF001KMI |
| H3K4me1 | ENCFF001KNF |
| LXR | GSM864669 |
| RXRα | GSM864674 |
| PPARα | GSM864671 |
| HNF4α | GSM2055887 |

893

894 Supplemental Table S4 is attached as an Excel file.

895

896 Supplemental Table S5. Primer sequences used in this study

897

898 A. List of primer sequences for mouse qRT-PCR

| Gene | Forward Primer (5'-3') | Reverse Primer (5'-3') |
|---|---|---|
| *FincoR* | GCAAAGCACCTTCTAGCACA | GTCAGGGAGCTAACGAATGC |
| *Gcnt1* | GCATCGCATCCTGCTTTGATA | GGTCTGCCTTAACCCGACTC |
| *Shp* | TCTGCAGGTCGTCCGACTAT | CAGGCAGTGGCTGTGAGAT |
| *Cyp7a1* | GGGATTGCTGTGGTAGTGAGC | GGTATGGAATCAACCCGTTGTC |

| | | |
|---|---|---|
| *Cyp8b1* | CCTCTGGACAAGGGTTTTGTG | GCACCGTGAAGACATCCCC |
| *Srebp1c* | GCAGCCACCATCTAGCCTG | CAGCAGTGAGTCTGCCTTGAT |
| *Lpin* | CATGCTTCGGAAAGTCCTTCA | GGTTATTCTTTGGCGTCAACCT |
| *Scd1* | TTCTTGCGATACACTCTGGTGC | CGGGATTGAATGTTCTTGTCGT |
| *Ifng* | GCG TCA TTG AAT CAC ACC TG | GAC CTG TGG GTT GTT GAC CT |
| *Ccl3* | TTCTCTGTACCATGACACTCTGC | CGTGGAATCTTCCGGCTGTAG |
| *Ccl2* | TTAAAAACCTGGATCGGAACCAA | GCATTAGCTTCAGATTTACGGGT |
| *Ccr2* | AAGAGGGCATTGGATTCACCACA | GCCGTGGATGAACTGAGGTAACA |
| *Lcn2* | GCAGGTGGTACGTTGTGGG | CTCTTGTAGCTCATAGATGGTGC |
| *Col1a1* | ATCGGTCATGCTCTCTCCAAACCA | ACTGCAACATGGAGACAGGTCAGA |
| *Col1a2* | CCTTTGTCAGAATACTGAGCAGC | GTAACTTCGTGCCTAGCAACA |
| *Acta2* | TCGGATACTTCAGCGTCAGGA | GTCCCAGACATCAGGGAGTAA |
| *Eda2r* | CACACTGCATAGTCTGCCCTC | GCCTTCTGGACCCGATTGA |
| *Fndc1* | GGGAGACATGGCAAACCTGT | TGGTAGGAGAGTATGTGGTGG |
| *Ctsb* | TCCTTGATCCTTCTTTCTTGCC | ACAGTGCCACACAGCTTCTTC |
| *Ctss* | GAAGTACGGCGTCTCATCTGG | CATGCCCACTTGGTAGGTATG |
| *Bcl2* | GTCGCTACCGTCGTGACTTC | CAGACATGCACCTACCCAGC |
| *36b4* | CCCTGAAGTGCTCGACATCA | TGCGGACACCCTCCAGAA |

## B. List of primers used for mutagenesis

| | Forward Primer (5'-3') | Reverse Primer (5'-3') |
|---|---|---|
| Mutation | GTGAATTCTCTCCTAGaTCcTTGACaTTCCAAGTC ATGTAC | GTACATGACTTGGAAtGTCAAgGAtCTAGGAGAGAATTC AC |

## C. List of primer sequences for mouse ChIP-qPCR

| **Gene** | **Forward Primer (5'-3')** | **Reverse Primer (5'-3')** |
|---|---|---|
| FincoR | TCCTAGGTCTTTGACCTTCCAA | TGTGCCCACTGGTGAAATAG |
| Non-specific region | GTGTACACGCCCAAACTTGA | GTTCACCTCTCTAGCTCACCT |

## D. List of primer used for RACE

| | **Gene specific primer (5'-3')** |
|---|---|
| 5'RACE | GATTACGCCAAGCTT GGGAACTCACGTCTGGAAGCAGAAGCTG |
| 3'RACE | GATTACGCCAAGCTT GGACACTCGGGAATTGACAGTGGGTCAGG |
| 3'RACE nest primer | GATTACGCCAAGCTT GTGGGGGATAGCACAAGCGCCAGGATGC |

907 E. List of primer used for genotyping

| Forward Primer (5'-3') | Reverse Primer (5'-3') |
|---|---|
| GTGATTTCCTTTCCCACAGC | GTCAGGGAGCTAACGAATGC |

908

Figure 1

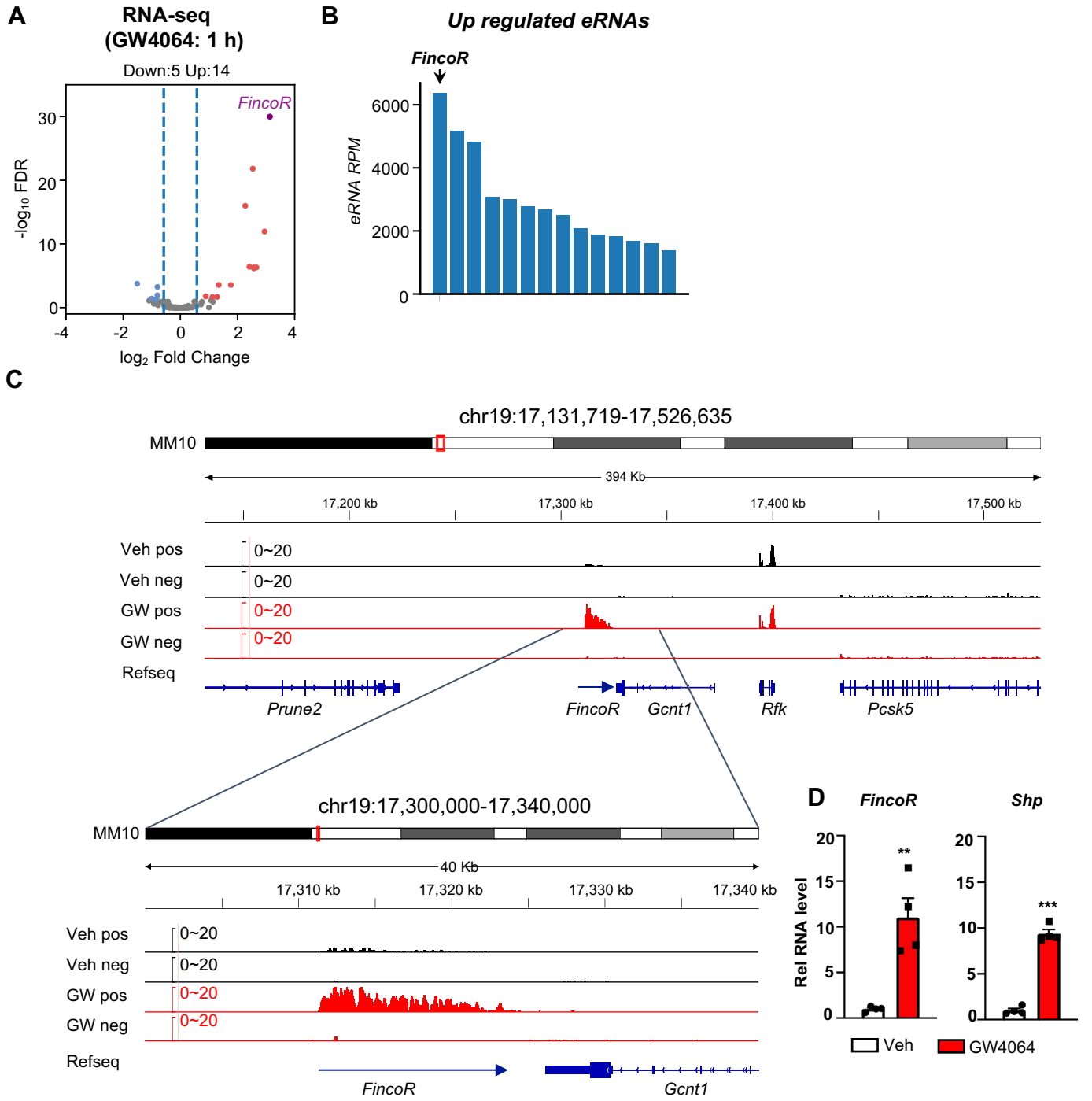
A
RNA-seq
(GW4064: 1 h)
Down:5 Up:14
FincoR
-log10 FDR
log2 Fold Change
B
Up regulated eRNAs
FincoR
eRNA RPM
C
chr19:17,131,719-17,526,635
MM10
394 Kb
17,200 kb
17,300 kb
17,400 kb
17,500 kb
Veh pos
Veh neg
GW pos
GW neg
Refseq
0~20
Prune2
FincoR
Gcnt1
Rfk
Pcsk5
chr19:17,300,000-17,340,000
40 Kb
17,310 kb
17,320 kb
17,330 kb
17,340 kb
D
FincoR
Shp
Rel RNA level
Veh
GW4064

Figure 2

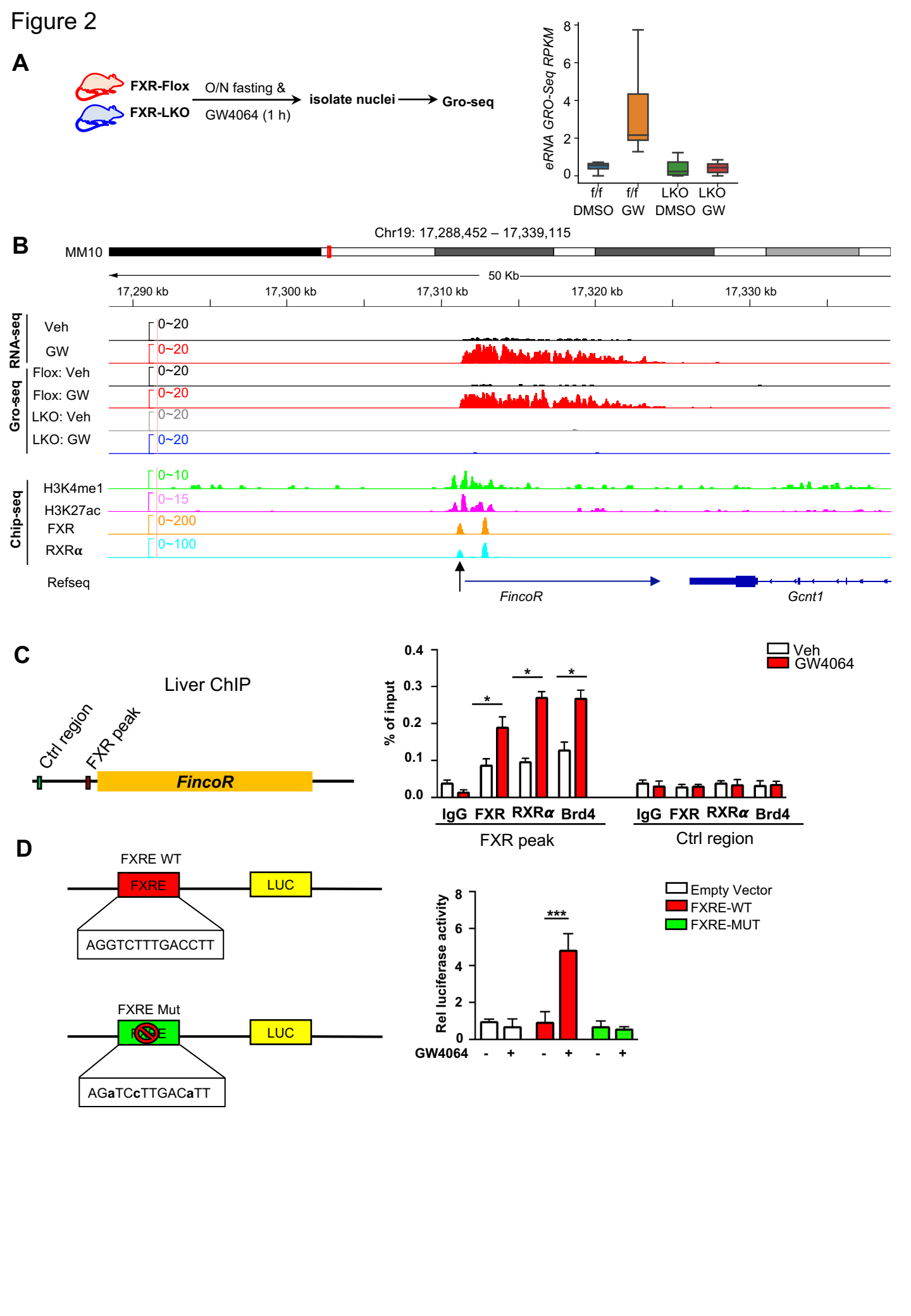
A
FXR-Flox
FXR-LKO
O/N fasting &
GW4064 (1 h)
isolate nuclei
Gro-seq
eRNA GRO-Seq RPKM
f/f DMSO
f/f GW
LKO DMSO
LKO GW
B
Chr19: 17,288,452 – 17,339,115
MM10
50 Kb
17,290 kb
17,300 kb
17,310 kb
17,320 kb
17,330 kb
RNA-seq
Veh
GW
Gro-seq
Flox: Veh
Flox: GW
LKO: Veh
LKO: GW
Chip-seq
H3K4me1
H3K27ac
FXR
RXRα
Refseq
FincoR
Gcnt1
C
Liver ChIP
Ctrl region
FXR peak
FincoR
Veh
GW4064
% of input
IgG FXR RXRα Brd4
FXR peak
Ctrl region
D
FXRE WT
FXRE
LUC
AGGTCTTTGACCTT
FXRE Mut
LUC
AGaTCcTTGACaTT
Empty Vector
FXRE-WT
FXRE-MUT
Rel luciferase activity
GW4064

Figure 3

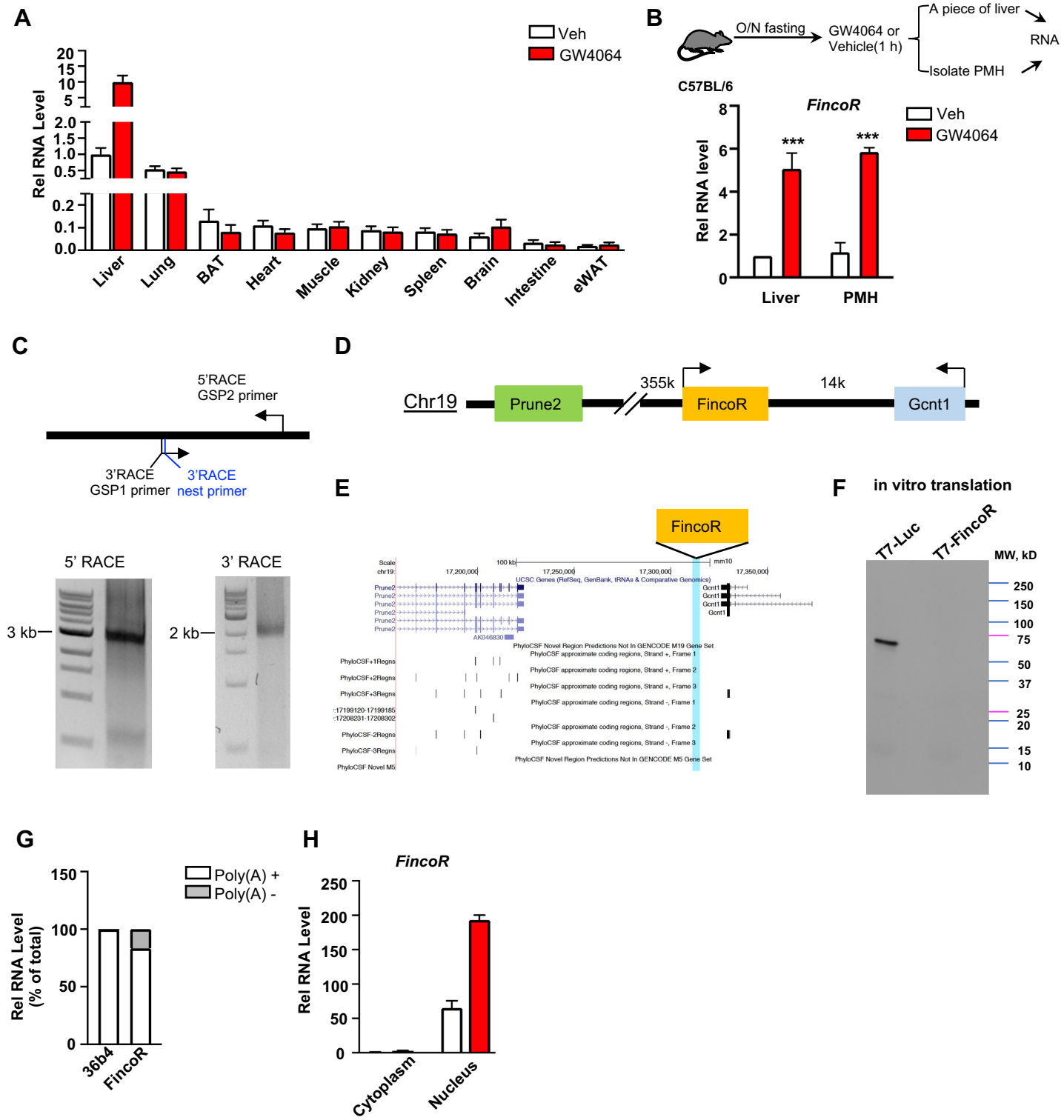
A
Veh
GW4064
Rel RNA Level
20
15
10
5
2.0
1.5
1.0
0.5
0.2
0.1
0.0
Liver
Lung
BAT
Heart
Muscle
Kidney
Spleen
Brain
Intestine
eWAT
B
O/N fasting
GW4064 or
Vehicle(1 h)
A piece of liver
Isolate PMH
RNA
C57BL/6
FincoR
Rel RNA level
***
***
Veh
GW4064
Liver
PMH
C
5'RACE
GSP2 primer
3'RACE
GSP1 primer
3'RACE
nest primer
5' RACE
3' RACE
3 kb
2 kb
D
Chr19
Prune2
355k
FincoR
14k
Gcnt1
E
FincoR
F
in vitro translation
T7-Luc
T7-FincoR
MW, kD
250
150
100
75
50
37
25
20
15
10
G
Poly(A) +
Poly(A) -
Rel RNA Level
(% of total)
150
100
50
0
36b4
FincoR
H
FincoR
Rel RNA Level
250
200
150
100
50
0
Cytoplasm
Nucleus

Figure 4

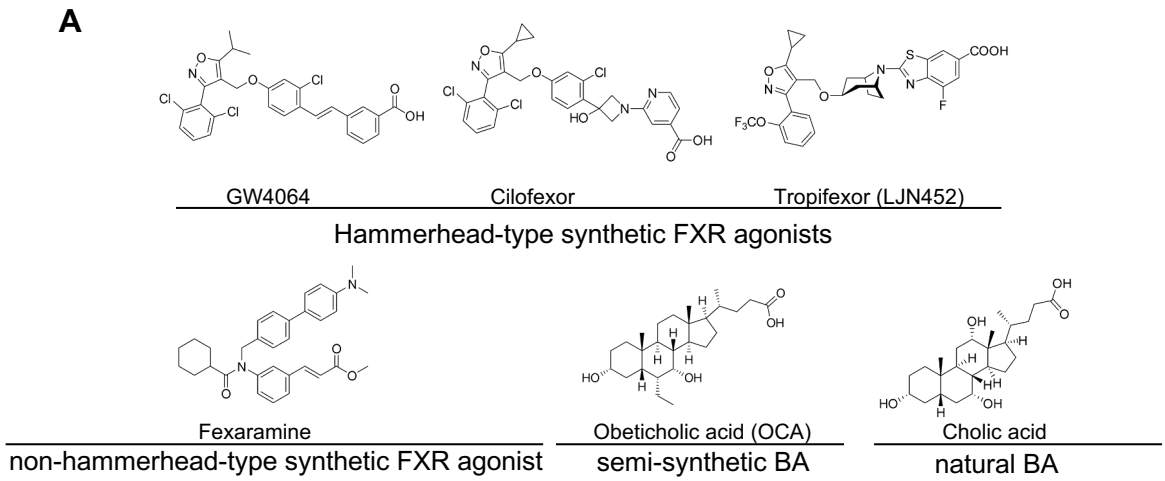
A
GW4064
Cilofexor
Tropifexor (LJN452)
Hammerhead-type synthetic FXR agonists
Fexaramine
non-hammerhead-type synthetic FXR agonist
Obeticholic acid (OCA)
semi-synthetic BA
Cholic acid
natural BA

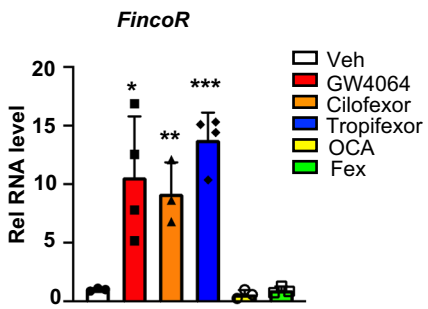
B
FincoR
Rel RNA level
Veh
GW4064
Cilofexor
Tropifexor
OCA
Fex

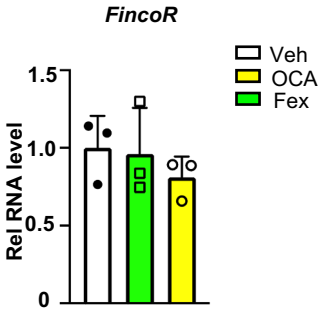
C
FincoR
Rel RNA level
Veh
OCA
Fex

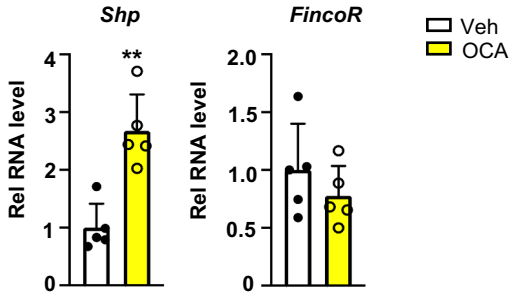
D
Shp
FincoR
Rel RNA level
Veh
OCA

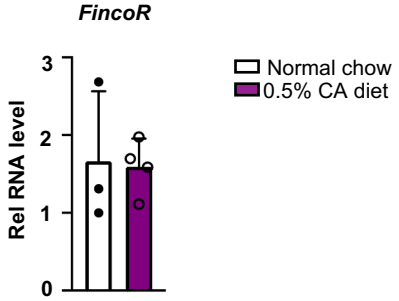
E
FincoR
Rel RNA level
Normal chow
0.5% CA diet

Figure 5

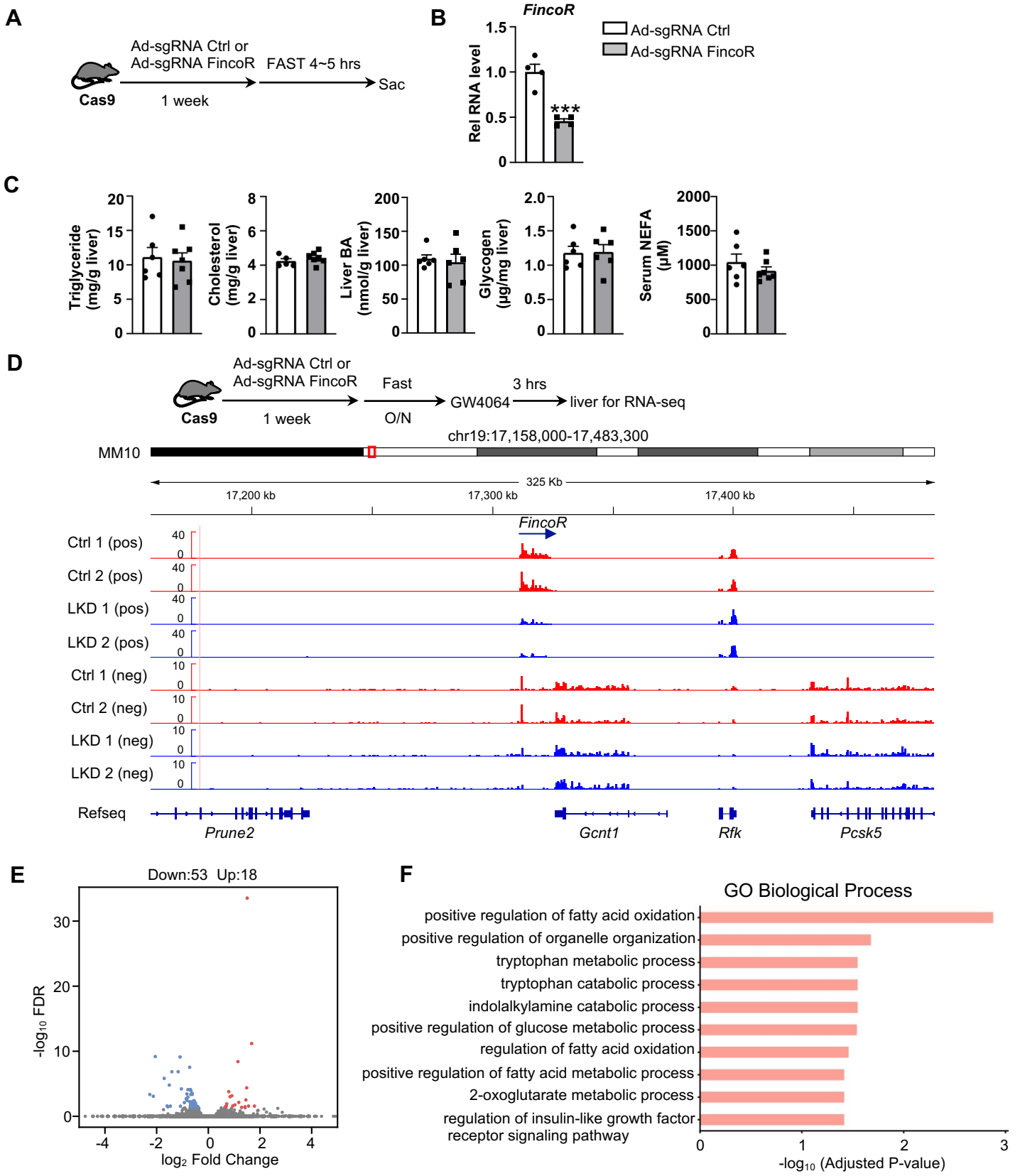
A
Cas9
Ad-sgRNA Ctrl or
Ad-sgRNA FincoR
1 week
FAST 4~5 hrs
Sac
B
FincoR
Rel RNA level
Ad-sgRNA Ctrl
Ad-sgRNA FincoR
***
C
Triglyceride (mg/g liver)
Cholesterol (mg/g liver)
Liver BA (nmol/g liver)
Glycogen (μg/mg liver)
Serum NEFA (μM)
D
Cas9
Ad-sgRNA Ctrl or
Ad-sgRNA FincoR
1 week
Fast
O/N
GW4064
3 hrs
liver for RNA-seq
MM10
chr19:17,158,000-17,483,300
325 Kb
17,200 kb
17,300 kb
17,400 kb
FincoR
Ctrl 1 (pos)
Ctrl 2 (pos)
LKD 1 (pos)
LKD 2 (pos)
Ctrl 1 (neg)
Ctrl 2 (neg)
LKD 1 (neg)
LKD 2 (neg)
Refseq
Prune2
Gcnt1
Rfk
Pcsk5
E
Down:53 Up:18
-log10 FDR
log2 Fold Change
F
GO Biological Process
positive regulation of fatty acid oxidation
positive regulation of organelle organization
tryptophan metabolic process
tryptophan catabolic process
indolalkylamine catabolic process
positive regulation of glucose metabolic process
regulation of fatty acid oxidation
positive regulation of fatty acid metabolic process
2-oxoglutarate metabolic process
regulation of insulin-like growth factor receptor signaling pathway
-log10 (Adjusted P-value)

Figure 6

Ad-sgRNA Ctrl + Veh | Ad-sgRNA Ctrl + Tropifexor | Ad-sgRNA FincoR + Tropifexor

A

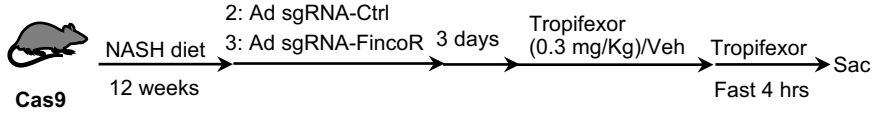


B

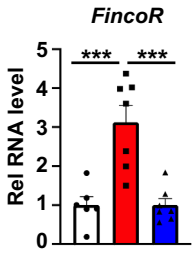


C

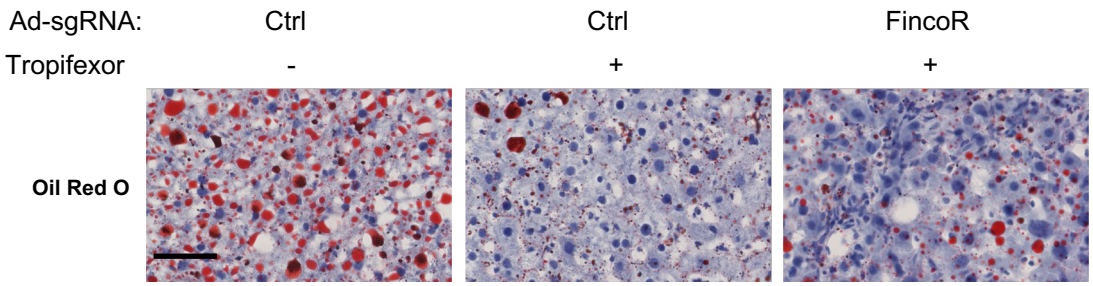


D

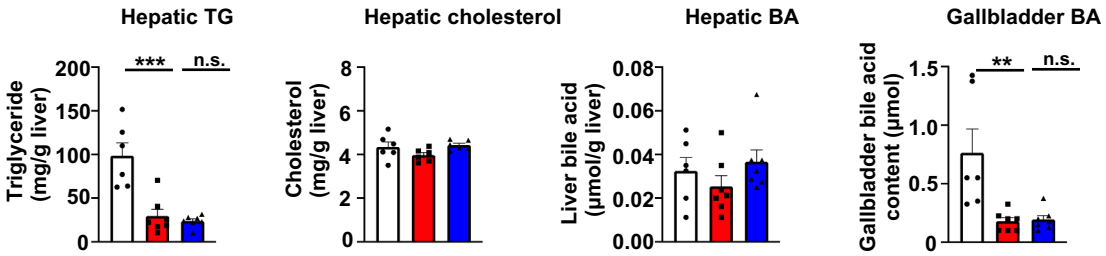


E

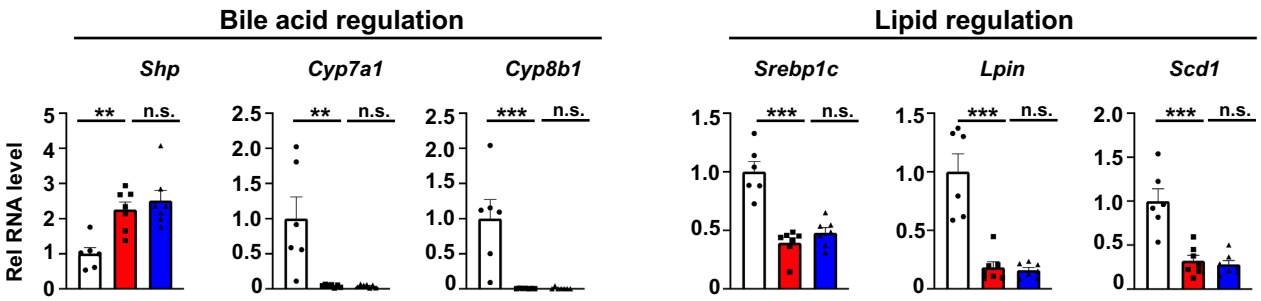


Ad-sgRNA Ctrl + Veh | Ad-sgRNA Ctrl + Tropifexor | Ad-sgRNA FincoR + Tropifexor

Figure 7

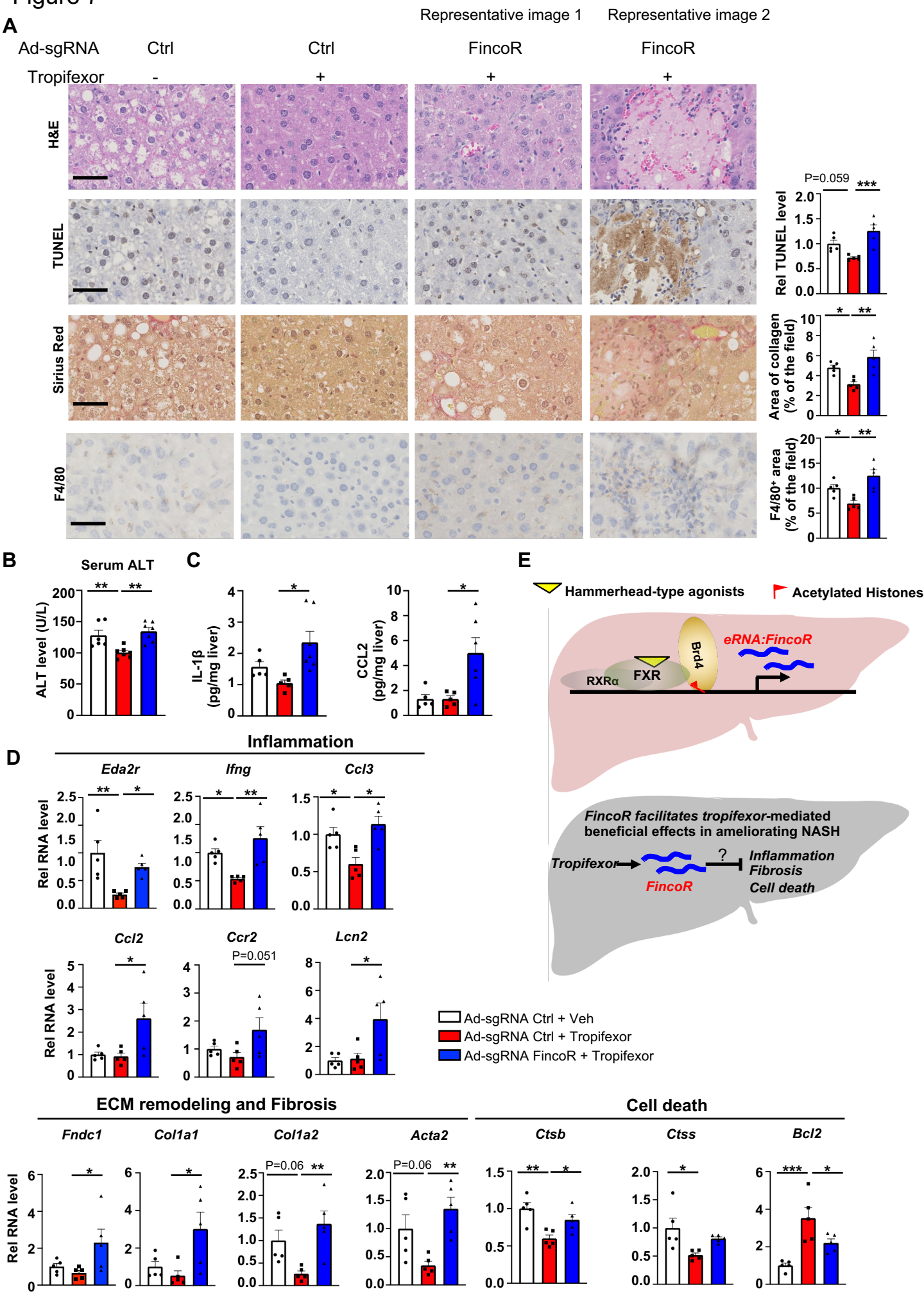
A
Representative image 1
Representative image 2
Ad-sgRNA
Ctrl
Ctrl
FincoR
FincoR
Tropifexor
-
+
+
+
H&E
TUNEL
Sirius Red
F4/80
P=0.059
***
Rel TUNEL level
*
**
Area of collagen (% of the field)
*
**
F4/80+ area (% of the field)
B
Serum ALT
ALT level (U/L)
C
IL-1β (pg/mg liver)
CCL2 (pg/mg liver)
E
Hammerhead-type agonists
Acetylated Histones
Brd4
eRNA:FincoR
RXRα
FXR
FincoR facilitates tropifexor-mediated beneficial effects in ameliorating NASH
Tropifexor
FincoR
?
Inflammation
Fibrosis
Cell death
D
Inflammation
Eda2r
Ifng
Ccl3
Ccl2
Ccr2
Lcn2
P=0.051
Rel RNA level
Ad-sgRNA Ctrl + Veh
Ad-sgRNA Ctrl + Tropifexor
Ad-sgRNA FincoR + Tropifexor
ECM remodeling and Fibrosis
Cell death
Fndc1
Col1a1
Col1a2
Acta2
Ctsb
Ctss
Bcl2
P=0.06
P=0.06

# Figure 1-Figure Supplement 1

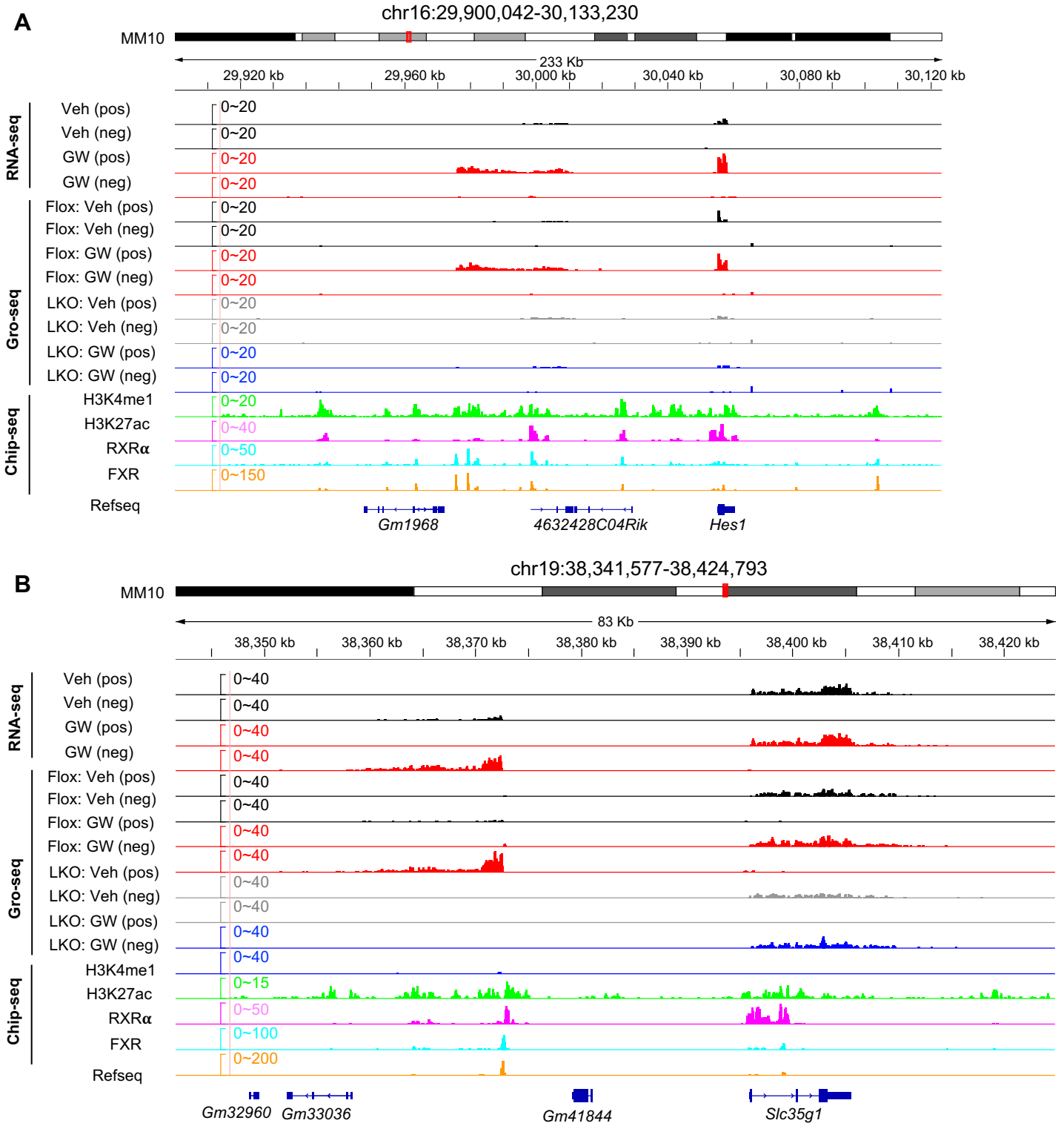

Figure 1–Figure Supplement 2

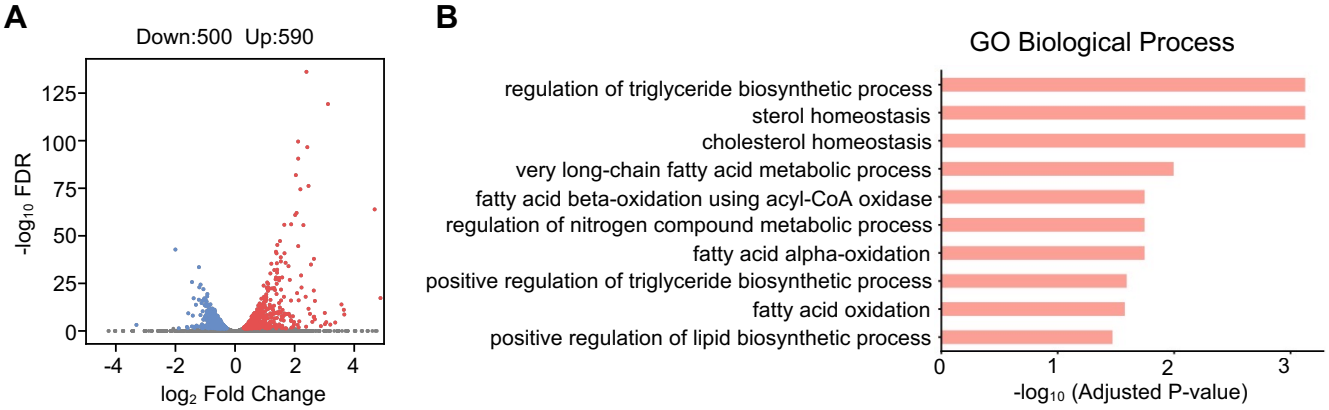

Figure 2-Figure Supplement 1

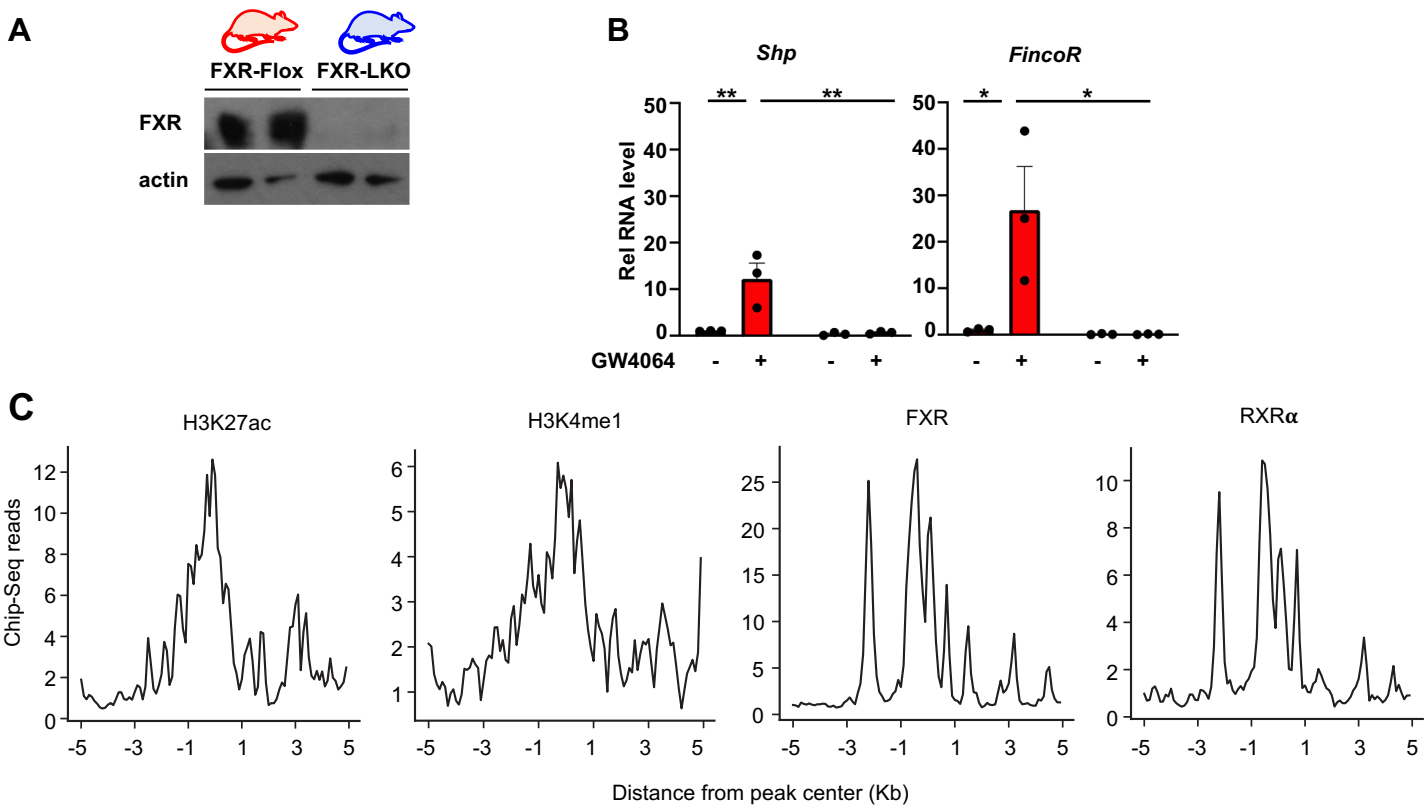

# Figure 5-Figure Supplement 1

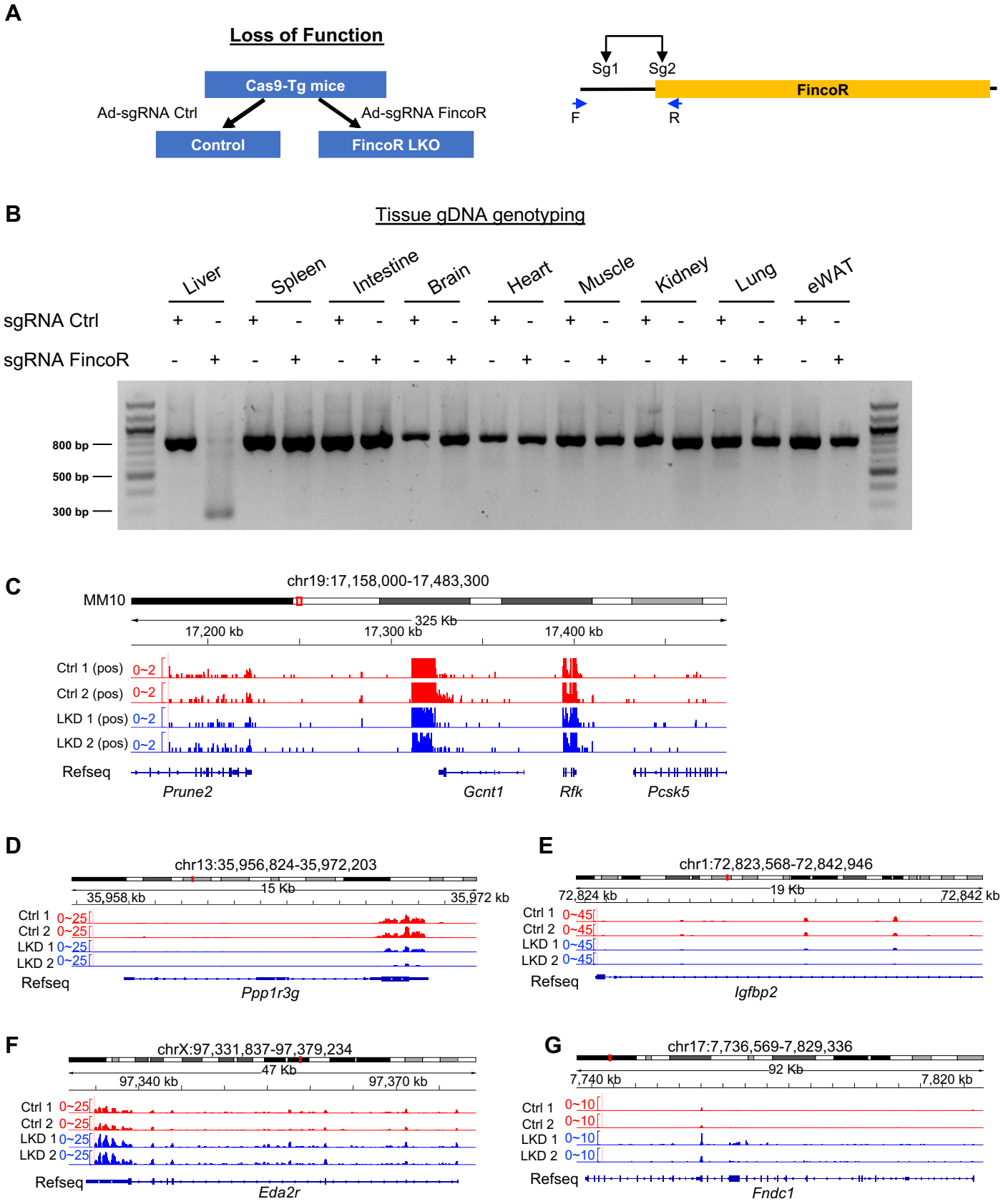

Figure 7-Figure Supplement 1

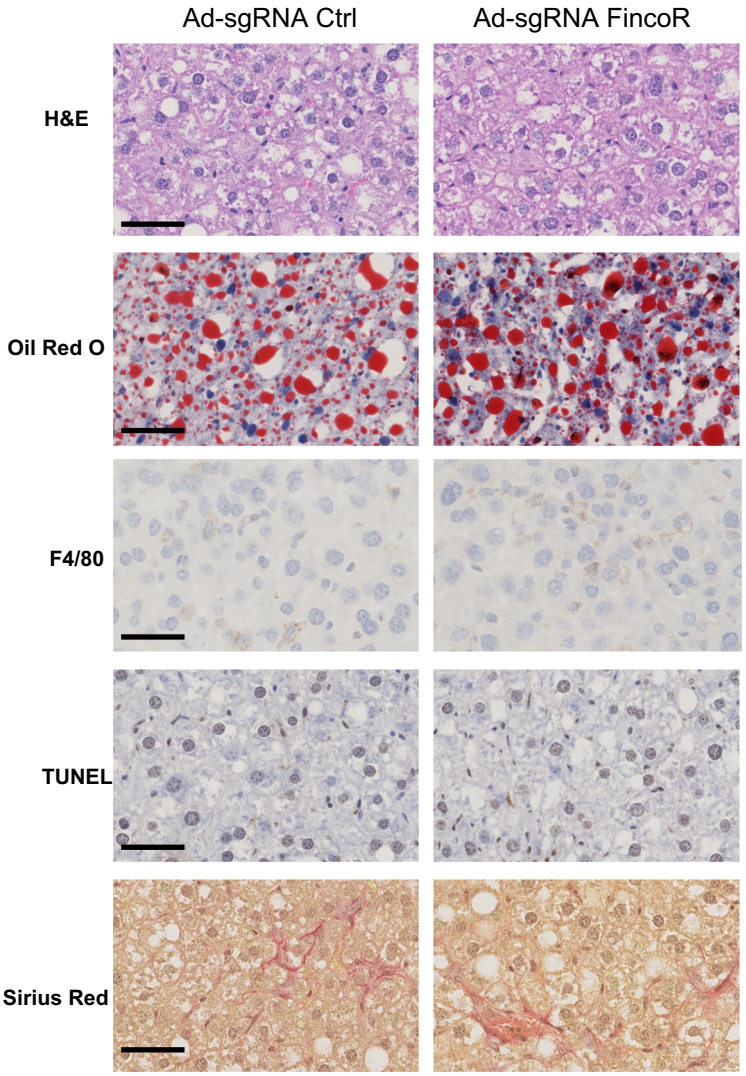

# Other Figure Supplement 1

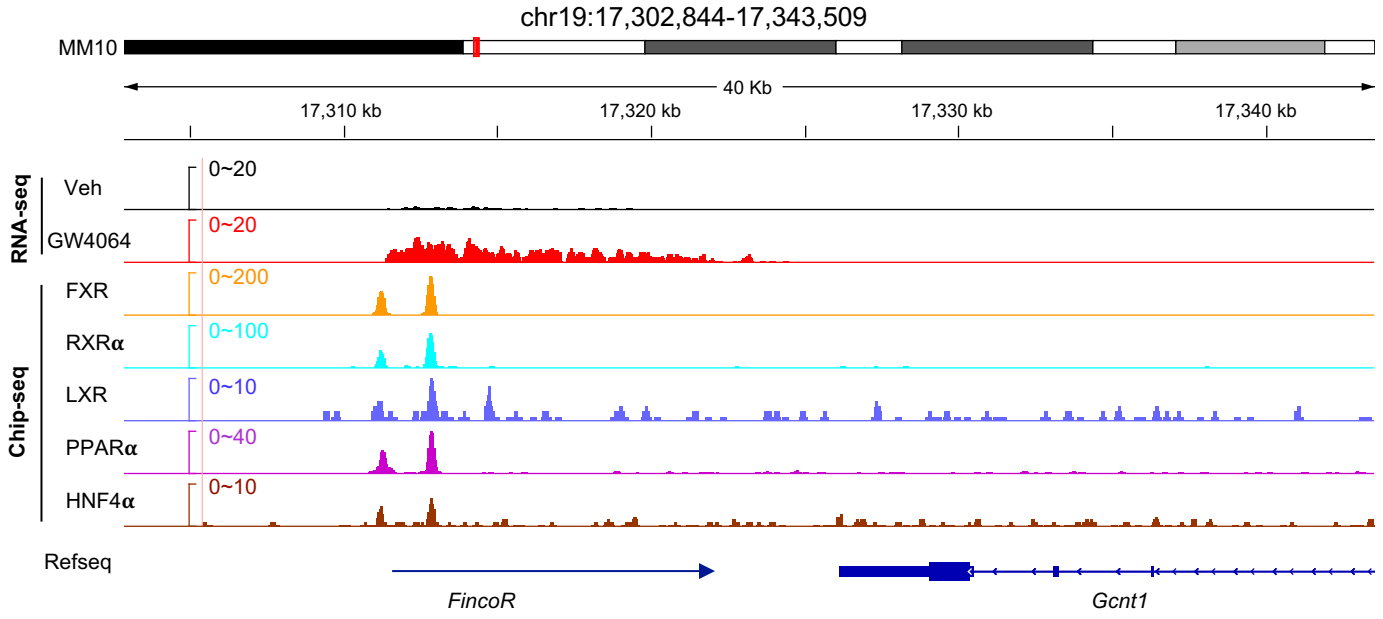
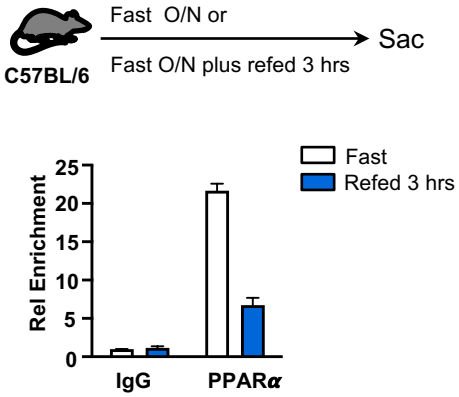
# Other Figure Supplement 2